



1 **Mapping the suitability of groundwater dependent**
2 **vegetation in a semi-arid Mediterranean area**

3

4 Inês Gomes Marques¹; João Nascimento²; Rita M. Cardoso¹; Filipe Miguéns²; Maria
5 Teresa Condesso de Melo²; Pedro M. M. Soares¹; Cathy Kurz Besson¹

6

7 ¹ Instituto Dom Luiz; Faculty of Sciences, University of Lisbon, Campo Grande, Ed. C8, 1749-016,
8 Lisbon, Portugal

9 ² CERIS; Instituto Superior Técnico, University of Lisbon, 1049-001, Lisbon, Portugal

10

11 *Correspondence to:* Inês Gomes Marques (icgmarques@fc.ul.pt)

12

13 **Abstract.** The forecasted groundwater resource depletion under future climatic conditions will greatly
14 influence groundwater dependent ecosystems and their associated vegetation. In the Mediterranean region
15 this will create harsh conditions for the maintenance of agroforestry systems dependent on groundwater,
16 such as cork oak woodlands. The threat of increasing aridity conditions will affect their productivity and
17 eventually induce a shift in their geographical distribution. Thus, characterizing and modelling the
18 relationship between environmental conditions and groundwater dependent vegetation (GDV) will allow
19 to identify the main drivers controlling its distribution and predict future impacts of climate change.

20 In this study, we built a model that explains the distribution of deep-rooted woody species in southern
21 Portugal from climatic, hydrological and topographic environmental variables. To achieve this, we relied
22 on the density of *Quercus suber*, *Quercus ilex* and *Pinus pinea* as proxy species of GDV. Model fitting
23 was performed between the proxy species Kernel density and the selected environmental predictors using
24 1) a simple linear model and 2) a Geographically Weighted Regression (GWR), to account for auto-
25 correlation of the spatial data and residuals. When comparing the results of both models, the GWR
26 modelling results showed improved goodness of fitting, as opposed to the simple linear model. Soil type
27 was the main driver of GDV density closely followed by the aridity index. Groundwater depth did not
28 appear to be as pertinent in the model as initially expected.

29 Model predictor coefficients were used as weighting factors for multicriteria analysis, to create a
30 suitability map to the GDV in southern Portugal. A validation of the resulting map was performed using
31 independent data of integrated potential distribution of each proxy tree species in the region and overall,
32 there was a good accordance between areas of good suitability to GDV. The model was considered
33 reliable to predict the distribution of the studied vegetation, however, lack of data quality and information
34 was shown to be the main cause for suitability discrepancies between maps.

35 Our new methodology on mapping of GDV's will allow to predict the evolution of the distribution of
36 GDV according to climate change scenarios and aid stakeholder decision-making concerning priority
37 areas of water resources management.



38

39 **Keywords:** Groundwater dependent ecosystems, aridity, agroforestry, suitability map

40

41



42 **1 Introduction**

43

44 Groundwater is the largest subsurface water reservoir and supports valuable ecosystems (Eamus et al.,
45 2006). Mediterranean forests, woodlands and shrublands, mostly growing under restricted water
46 availability, are one of the terrestrial biomes with higher volume of groundwater used by vegetation
47 (Evaristo and McDonnell, 2017). Future predictions of decrease precipitation (Giorgi and Lionello, 2008;
48 Nadezhdina et al., 2015), decreased runoff (Mourato et al., 2015) and aquifer recharge (Ertürk et al.,
49 2014) in the Mediterranean region threaten the sustainability of groundwater reservoirs and the
50 corresponding dependent ecosystems. Therefore, a sustainable management of groundwater resources and
51 the Groundwater Dependent Ecosystems (GDE) is of crucial importance.

52 Mapping GDE constitutes a first and fundamental step to their active management. Several approaches
53 have been proposed, including remote sensing techniques (e.g. Normalized Difference Vegetation Index –
54 NDVI) (Barron et al., 2014; Eamus et al., 2015; Howard and Merrifield, 2010), remote-sensing combined
55 with ground-based observations (Lv et al., 2013), based on geographic information system (GIS) (Pérez
56 Hoyos et al., 2016a) or statistical approaches (Pérez Hoyos et al., 2016b). Integrated multidisciplinary
57 methodology (Condesso de Melo et al., 2015) has also been used. A widely used classification of GDE
58 was proposed by Eamus et al. (2006). This classification distinguishes between three types: 1) Aquifer
59 and cave ecosystems, which includes all subterranean waters; 2) Ecosystems reliant on surface
60 groundwater (e.g. estuarine systems, wetlands; riverine systems) and 3) Ecosystems reliant on subsurface
61 groundwater (e.g. systems where plants remain physiologically active during extended drought periods,
62 without visible water source).

63 Despite of a wide-ranging body of literature regarding GDE, most of the studies did not included
64 Mediterranean regions (Doody et al., 2017; Dresel et al., 2010; Münch and Conrad, 2007). Moreover,
65 studies on ecosystems relying on subsurface groundwater frequently only focused on riparian
66 environments (Lowry and Loheide, 2010; O’Grady et al., 2006), with few examples in Mediterranean
67 areas (del Castillo et al., 2016; Fernandes, 2013; Hernández-Santana et al., 2008; Mendes et al., 2016).
68 There is a clear knowledge gap concerning the identification of such ecosystems, their phreatophyte
69 associated vegetation (Robinson, 1958) in the Mediterranean region and the management actions that
70 should be taken to decrease the adverse effects of climate change.

71 In the driest regions of the Mediterranean basin, the persistent lack of water during the entire summer
72 periods selected plants with drought-avoiding strategies, like those that reach deeper stored water up to
73 the point of relying on groundwater (Canadell et al., 1996; Miller et al., 2010). Groundwater access by
74 deep rooting species is often associated to hydraulic lift and/or hydraulic redistribution mechanisms
75 (Orellana et al., 2012). Those mechanisms provide the ability to move water from deep soil layers, where
76 water content is higher, to more shallow layers where water content is lower (Horton and Hart, 1998;
77 Neumann and Cardon, 2012). Hydraulic lift and redistribution have been reported for several woody
78 species of the Mediterranean basin (David et al., 2007; Filella and Peñuelas, 2004) and noticeably for
79 Cork oak (*Quercus suber* L.) (David et al., 2013; Kurz-Besson et al., 2006; Mendes et al., 2016).



80 Cork oak woodlands are agro-silvo-pastoral systems of the southwest Mediterranean basin (Joffre et al.,
81 1999) who have already been referenced as a groundwater dependent terrestrial ecosystem (Mendes et
82 al., 2016). In the ecosystems of this geographical area, the dominant tree species are the cork oak
83 (*Quercus suber* L.) and the Portuguese holm oak (*Quercus ilex* subs *rotundifolia* Lam.) (Pinto-Correia et
84 al., 2011). Additionally, stone pine (*Pinus pinea* L.) has become a commonly co-occurrent species in the
85 last decades (Coelho and Campos, 2009). The use of groundwater has been frequently reported for both
86 *Pinus* (Filella and Peñuelas, 2004; Grossiord et al., 2016; Peñuelas and Filella, 2003) and *Quercus*
87 (*Barbeta and Peñuelas, 2017; David et al., 2007, 2013, Kurz-Besson et al., 2006, 2014; Otieno et al.,*
88 *2006*) genders. Furthermore, the contribution of groundwater to tree physiology has been shown to be of a
89 greater magnitude for *Quercus* sp. as compared with *Pinus* sp. (del Castillo et al., 2016; Evaristo and
90 McDonnell, 2017).

91 *Q. suber* and *Q. ilex* have been associated with high resilience and adaptability to hydric and thermic
92 stress, and to recurrent droughts in the southern Mediterranean basin (Barbero et al., 1992). In Italy and
93 Portugal, during summer droughts *Q. ilex* used a mixture of rain-water and groundwater and was able to
94 take water from very dry soils (David et al., 2007; Valentini et al., 1992). An increasing contribution of
95 groundwater in the summer has also been shown for this species (Barbeta et al., 2015). Similarly, *Q.*
96 *suber* showed a seasonal shift in water sources, from shallow soil water in the spring to the beginning of
97 the dry period followed by a progressive higher use of deeper water sources throughout the drought
98 period (Otieno et al., 2006). In addition, the species roots are known to reach depths as deep as 13m in
99 southern Portugal (David et al., 2004). Although co-occurrent to cork and holm oaks species, there is still
100 no evidence yet that *P. pinea* relies on groundwater resources during the dry season. However it shows a
101 very similar root system (Montero et al., 2004) as compared to cork oak (David et al., 2013), with large
102 sinker roots reaching 5m depth (Canadell et al., 1996). Given the information available on water use
103 strategies by the phreatophyte arboreal species of the cork oak woodlands, we considered *Q. ilex*, *Q.*
104 *suber* and *P. pinea* as proxies for vegetation that belongs to GDE relying on subsurface groundwater
105 (from here onwards designed as Groundwater Dependent Vegetation – GDV).

106 GDV of the Mediterranean basin is often neglected in research. Indeed, still little is known about the
107 GDV distribution, but research has already been done on the effects of climate change in specific species
108 distribution, such as *Q. suber*, in the Mediterranean basin (Duque-Lazo et al., 2018; Paulo et al., 2015).
109 While the increase in atmospheric CO₂ and the raising temperature can boost tree growth (Barbeta and
110 Peñuelas, 2017; Bussotti et al., 2013; Sardans and Peñuelas, 2004), water stress can have a counteracting
111 effect on growth of both *Quercus ilex* (López et al., 1997; Sabaté et al., 2002) and *P. pinaster* (Kurz-
112 Besson et al., 2016). Therefore, it is of crucial importance to identify geographical areas where subsurface
113 GDV is present and characterize the environmental conditions this vegetation type is thriving in. This
114 would contribute to the understanding of how to manage these species under unfavorable future climatic
115 conditions.

116 The aim of this study was to create a suitability map of the current distribution of GDV in southern
117 Portugal, based on the occurrence of known and foreseen subsurface phreatophyte species and well-
118 known environmental conditions affecting groundwater storage. Several environmental predictors were



119 selected according to their impact on groundwater use and storage and then used in a Geographically
120 Weighted Regression (GWR) to model the density of *Q. suber*, *Q. ilex* and *P. pinea* occurrence in the
121 Alentejo region (NUTSII) of southern Portugal. So far, very few applications of this method have been
122 used to model species distribution and only recently its use has spread in ecological research (Hu et al.,
123 2017; Li et al., 2016; Mazziotta et al., 2016). The coefficients obtained from the model equation for each
124 predictor were used as weights to build the suitability map with GIS multi-factor analysis, after
125 reclassifying each environmental predictor.

126 Based on the environmental conditions of the study area and the species needs, we hypothesized that 1)
127 groundwater depth together with climatic conditions play one of the most important environmental roles
128 in GDV's distribution and 2) a more superficial access to groundwater and less arid conditions should
129 allow a higher density of GDV. Therefore, a higher suitability should be expected under such conditions.

130 We start by presenting the methodology used to create the environmental variables for the study area of
131 Alentejo, followed by an explanation of how the model was constructed and lead to the GDV suitability
132 map and subsequent validation. In the result section in chapter 3, we display the maps for the
133 environmental variables and parameters from the model fitting, the final suitability map and respective
134 validation. The results are discussed in the fourth chapter and the conclusions are presented in the fifth
135 chapter.

136

137



138 **2 Material and Methods**

139

140 **2.1 Study area**

141 The administrative region of Alentejo (NUTSII) (fig01) covers an area of 31 604.9 km², between the
142 latitude 37.22° to 39.39° N and longitude 9.00° to 6.55° W. This study area is characterized by a
143 Mediterranean temperate mesothermic climate with hot and dry summers, defined as Csa in the Köppen
144 classification (APA, n.d.; ARH Alentejo, 2012a, 2012b). It is characterized by a sub-humid climate,
145 which has recently quickly drifted to semi-arid conditions (Ministério da Agricultura do Mar do
146 Ambiente e do Ordenamento do Território, 2013). A large proportion of the area (above 40%) is covered
147 by forestry systems (Autoridade Florestal Nacional and Ministério da Agricultura do Desenvolvimento
148 Rural e das Pescas, 2010) providing a high economical value to the region and the country (Sarmiento and
149 Dores, 2013).

150

151 **2.2 Kernel Density estimation of GDV**

152 Presence datasets of *Quercus suber*, *Quercus ilex* and *Pinus pinea* of the last Portuguese forest inventory
153 achieved in 2010 (ICNF, 2013) were used to calculate Kernel density (commonly called heat map) as a
154 proxy to GDV suitability. Only data points with one of the three proxy species selected as primary and
155 secondary occupation were used. The resulting Kernel density was weighted according to tree cover
156 percentage and was calculated using a quartic biweight distribution shape, a search radius of 10km, and
157 an output resolution of 0.018 degrees, corresponding to a cell size of 1 km. This variable was computed
158 using QGIS version 2.14.12 (QGIS Development Team, 2017).

159

160 **2.3 Environmental variables**

161 Species distribution is mostly affected by limiting factors (controlling ecophysiological responses),
162 disturbances and resources (Guisan and Thuiller, 2005). To characterize the study area in terms of GDV
163 suitability, environmental variables expected to affect GDV's density were selected according to their
164 constraint on groundwater uptake and soil water storage. Within possible abiotic variables, landscape
165 topography, geology, groundwater availability and regional climate were considered to map GDV density
166 in the study area. The twelve selected variables for modeling purposes, retrieved from different data
167 sources are listed on Table 1.

168

169 **2.3.1 Topography and Geology**

170 NASA and METI ASTER GDEM product (<https://lpdaac.usgs.gov>) was retrieved from the online Data
171 Pool. Spatial Analyst Toolbox from ArcGIS® software version 10.4.1 by Esri was used to calculate the



172 slope from the digital elevation model. Slope was used as proxy for the identification of superficial water
173 interaction with vegetation.

174 The map of soil type was obtained from the Portuguese National Information System for the Environment
175 - SNIAmb (© Agência Portuguesa do Ambiente, I.P., 2017) and uniformized to the World Reference
176 Base with the Harmonized World Soil Database v 1.2 (FAO et al., 2009). The vector map was converted
177 to raster using the Conversion Toolbox from ArcGIS® software version 10.4.1 by Esri. To reduce the
178 analysis complexity involving the several soil types present in the map, soil types were regrouped in three
179 classes, according to their capacity to store or drain water. The classification was based on the
180 characteristics of each soil unit (available water storage capacity, drainage and topsoil texture) from the
181 Harmonized World Soil Database (FAO et al., 2009).

182 Effective soil thickness (Table 1) represents the maximum soil depth explored by the vegetation roots. It
183 constrains the expansion and growth of the root system, as well as the available amount of water that can
184 be absorbed by roots.

185

186 **2.3.2 Groundwater availability**

187 Root access to groundwater is one of the most limiting factors for GDV's growth and survival, especially
188 during the dry season. The map of depth to water table was interpolated from piezometric observations
189 from the Portuguese National Information System on Water Resources (SNIRH) public data base
190 (<http://snirh.apambiente.pt>, last accessed on March 31st 2017) and the Study of Groundwater Resources of
191 Alentejo (ERHSA) (Chambel et al., 2007). Data points of large-diameter wells and piezometers were
192 retrieved for the Alentejo region (fig02) and sorted into undifferentiated, karst or porous geological types
193 to model groundwater depth. Due to the large heterogeneity of geological media, groundwater depth was
194 calculated separately for each sub-basin. A total of 3158 data points corresponding to large wells and
195 piezometers were used, with uneven measurements between 1979 and 2017. For each piezometer an
196 average depth was calculated from the available observations and used as a single value. In areas with
197 undifferentiated geological type, piezometric level and elevation were highly correlated (>0.9), thus a
198 linear regression was applied to interpolate data. Ordinary kriging was preferred for the interpolation of
199 karst and porous aquifers, combining large wells and piezometric data points. To build a surface layer of
200 the depth to water table, the interpolated surface of the groundwater level was subtracted from the digital
201 elevation model. Geostatistical Analyst ToolBox from ArcGIS® software version 10.4.1 by Esr was used
202 for this task.

203 Drainage density is a measure of how well the basin is drained by stream channels. It is defined as the
204 total length of channels per unit area. Drainage density was calculated for each of the six hydrographic
205 basins of the Alentejo region, by the division between the total stream length (L) in km and the basin area
206 (A) in km², as in Eq. (1).

$$207 \quad Dd = \frac{L}{A}, \quad (1)$$



208

209 **2.3.3 Regional Climate**

210 Temperature and precipitation datasets were obtained from the E-OBS

211 (<http://eca.knmi.nl/download/ensembles/ensembles.php>, last accessed on March 31st 2017) public

212 database (Haylock et al., 2008). Standardized Precipitation Evapotranspiration Index (SPEI), Aridity

213 Index (AI) and Ombrothermic Indexes were computed from long-term (1951-2010) monthly temperature

214 and precipitation observations. The computation of potential evapotranspiration (PET) was performed

215 according to Thornthwaite (1948) and was assessed using the SPEI package (Beguería and Vicente-

216 Serrano, 2013) in R program software version 3.4.2 (R Development Core Team, 2016).

217 SPEI multi-scalar drought index (Vicente-Serrano et al., 2010) was calculated over a 6 month interval to

218 characterize drought severity in the area of study using SPEI package (Beguería and Vicente-Serrano,

219 2013) for R program. SPEI is based on the normalization of the water balance calculated as the difference

220 between cumulative precipitation and PET for a given period at monthly intervals. Normalized values of

221 SPEI typically range between -3 and 3. Drought events were considered as severe when SPEI values were

222 between -1.5 and -1.99, and as extreme with values below -2 (Mckee et al., 1993). Severe and extreme

223 SPEI predictors were computed as the number of months with severe or extreme drought, counted along

224 the 60 years of the climate time-series.

225 Aridity index gives information related to evapotranspiration processes and rainfall deficit for potential

226 vegetative growth. It was calculated following Eq. (2) according to Middleton et al. (1992), where PET is

227 the average annual potential evapotranspiration and P is the average annual precipitation, both in mm for

228 the 60 years period of the climate time-series. Dry lands are defined by their degree of aridity in 4 classes:

229 Hyperarid ($AI < 0.05$); Arid ($0.05 < AI < 0.2$); Semi-arid ($0.2 < AI < 0.5$) and Dry Subhumid ($0.5 < AI < 0.65$)

230 (Middleton et al., 1992).

231
$$AI = \frac{P}{PET}, \quad (2)$$

232 Ombrothermic Indexes were used to better characterize the bioclimatology of the study region (Rivas-

233 Martínez et al., 2011), by evaluating soil water availability for plants during the driest months of the year.

234 Four ombrothermic indexes were calculated following Eq. (3), where Pp is the positive annual

235 precipitation (accumulated monthly precipitation when the average monthly mean temperature is higher

236 than 0°C) and Tp is the positive annual temperature (total in tenths of degrees centigrade of the average

237 monthly temperatures higher than 0°). If the ombrothermic index presents values above 2 for the analyzed

238 months, the area cannot be considered as Mediterranean bioclimatically. For non-Mediterranean areas,

239 there is no dry period in which, for at least two consecutive months, the precipitation is less than or equal

240 to twice the temperature. Each ombrothermic index differed in the examined period of the year (Table1).

241
$$Io = \frac{Pp}{Tp}, \quad (3)$$

242

243 **2.4 Predictors selection**



244 The full set of environmental variables were evaluated as potential predictors for the suitability of GDV
245 (based on the Kernel density of the proxy species). A preliminary selection was carried out, first by
246 computing Pearson's correlation coefficients between environmental variables and second by performing
247 a Principal Components Analysis (PCA) to detect multicollinearity. Covariates were discarded for
248 modeling according to a sequential procedure. Whenever pairs of variables presented a correlation value
249 above 0.4, the variable with the highest explained variance on the first axis of the PCA was selected.
250 Variables showing low correlations and explaining a higher cumulative proportion of variability with the
251 lowest number of PCA axis were later selected as predictors for modeling. PCA was performed using the
252 GeoDa Software (Anselin et al., 2006) and Pearson's correlation coefficients were computed with Spatial
253 Analyst Tool from ArcGIS ® software version 10.4.1 by Esri.

254

255 **2.5 Model development**

256 When fitting a linear regression model to the selected variables, we must assure a normal distribution and
257 stationarity of the model residuals. However, spatial autocorrelation and non-stationarity are common
258 when using linear regression on spatial data. To overcome these issues, Geographically Weighted
259 Regression (GWR) was used to allow model coefficients to adjust to each location of the dataset, based
260 on the proximity of sampling locations (Stewart Fotheringham et al., 1996). In this study, simple linear
261 regression and GWR were both applied to the dataset and their performances compared. Models were
262 fitted on a 5% random subsample of the entire dataset (6242 data points), due to computational
263 restrictions.

264 Adaptive Kernel bandwidths for the GWR model fitting were used due to the spatial irregularity of the
265 random subsample. Bandwidths were obtained by minimizing the CrossValidation score (Bivand et al.,
266 2008). To analyze the performance of the GWR model alone, the local and global adjusted R-squared
267 were considered. To compare between the GWR model and the simple linear model, we considered the
268 distribution of the model residuals, e.g. whether there were visible clustered values. The second-order
269 Akaike Information Criterion (AICc) was also contemplated. The spatial autocorrelation of the models
270 residuals was evaluated with the Moran's I test (Moran, 1950) using the Spatial Statistics Tool from
271 ArcGIS ® software version 10.4.1 by Esri, and also graphically. GWR model was fitted using the *spgwr*
272 package from R program version 3.4.2 (Bivand and Yu, 2017).

273

274 **2.6 Suitability map building**

275 To create the suitability map we proceeded with the classification of all predictor layers included in the
276 GWR model, similarly to Condesso de Melo et al. (2015) and Aksoy et al. (2017). The likelihood of an
277 interaction between the vegetation and groundwater resources was scored from 0 to 3 for each predictor.
278 Scores were assigned after bibliographic review and expert opinion. The higher the score, the higher the
279 likelihood, 1 corresponding to a weak likelihood and 3 indicating very high likelihood. Groundwater
280 depth was divided in two classes, according to the accessibility to superficial water above 1.5m and the
281 maximum rooting depth for Mediterranean woody species reaching 13 m, reported by Canadell et al.



282 (1996). The minimum score was given to areas where groundwater depth was too shallow (below 1.5m).
283 This allowed to identify species dependent on more superficial groundwater which were considered to
284 belong to other types of groundwater dependent vegetation. Areas with steep slope were considered to
285 have superficial water flow (e.g. areas with permanent water table close to the surface due to proximity to
286 permanent streams) and influence negatively tree density (Costa et al., 2008). Those areas were treated as
287 less suitable to GDV. Aridity Index and Ombrothermic Index of the summer quarter and the immediately
288 previous month (Ios4) values were split in 3 classes according to Jenks natural breaks, with higher
289 suitability scores corresponding to higher aridity.

290 A direct compilation of the predictor layers could have been performed, however not all predictors
291 influence in the same measure the distribution of this type of vegetation. Therefore, there was a need to
292 define weighting factors for each layer of the final GIS multicriteria analysis. Yet, due to the intricate
293 relations between all environmental predictors and their effects on the GDV, experts and stakeholders
294 provided very different scoring for a same layer. Subsequently, we instead chose to use the coefficients of
295 the GWR model (Eq. 4) as weighting factors. The final GIS multicriteria analysis was performed using
296 the Spatial Analyst Tool ArcGIS® software version 10.4.1 by Esri, resulting in the final suitability map.

297 In the latter, lower values indicate a lower probability of GDV occurrence while higher values correspond
298 to a higher suitability. To allow for an easier interpretation, the data on suitability to GDV was
299 subsequently classified based on their distribution value, according to Jenks natural breaks. This resulted
300 in 5 suitability classes: “Very poor”, “Poor”, “Moderate”, “Good” and “Very Good”.

301

302 2.7 Map validation

303 To assess the quality of the suitability map obtained in the present study, independent maps of integrated
304 suitability to *Q. suber*, *Q. ilex* and *P. Pinea* were retrieved from the EPIC WebGIS Portugal ([http://epic-
305 webgis-portugal.isa.ulisboa.pt/](http://epic-webgis-portugal.isa.ulisboa.pt/)) public data base (Magalhães et al., 2015a, 2015b, 2015c). Those
306 distribution maps represent the suitability to a tree species according to bioclimatic, soil morphological
307 conditions and best silvicultural practices (Magalhães et al., 2015a). By overlapping the maps of the three
308 species in ArcGIS, we obtained a synthetic independent map where it was possible to identify suitable
309 areas to none, one, two or three of the tree species, considered good proxies of GDV (fig. C1).

310 Artificialized areas, rocky outcrops, rivers and humid areas were eliminated from the evaluation and
311 validated maps before performing an analytical comparison using the Analysis Tool ArcGIS® software
312 version 10.4.1 by Esri.

313

314



315 3 Results

316

317 3.1 Kernel Density

318 Within the studied region of Portugal, the phreatophyte species *Quercus suber*, *Quercus ilex* and the
319 suspected phreatophyte species *Pinus pinea* were not distributed uniformly throughout the territory. Areas
320 with higher Kernel density (or higher distribution likelihood) were mostly spread between the northern
321 part of Alentejo region and the western part close to the coast, with values ranging between 900 and 1200
322 (fig03). Two clusters of high density also appeared below the Tagus river. The remaining study area
323 presented mean density values, with a very low density in the area of the river Tagus.

324

325 3.2 Environmental conditions

326 The exploratory analysis of the variables, performed through the PCA and Pearson correlation matrix
327 confirmed the presence of multicollinearity. From the initial variables (Table 1), Thickness, Drainage
328 Density, Spei_severe, Spei_extreme, Annual Ombrothermic Index (Io), Ombrothermic Index of the
329 hottest month of the summer quarter (Ios1) and Ombrothermic Index of the summer quarter (Ios3) were
330 discarded, while the variables slope, soil type, depth, AI and Ios4 were maintained for analysis (fig. A1
331 and Table A1 in appendix). Therefore, five environmental variables out of the initial 12 considered
332 (fig04) were endorsed to explain the variation of the Kernel density of GDV in Alentejo: soil type,
333 ombrothermic index of the summer quarter and the immediately previous month (ios4), slope, aridity
334 index and groundwater depth.

335 The Alentejo region showed high heterogeneity of soil types, with 27 different categories (fig04a). In
336 most part of the region, slope was below 10% (fig04b), coastal areas presenting the lowest values and
337 variability. Highest values of groundwater depth (fig04c), reaching a maximum of 255m, were found in
338 the Atlantic margin of the study area, mainly in Tagus and Sado river basins. Several other small and
339 confined areas in Alentejo also showed high values, corresponding to aquifers of porous or karst
340 geological types. Most of the remaining study area showed groundwater depths ranging between 1.5m
341 and 15m. Figures 4d and 4e indicate the southeast of Alentejo as the driest area, given by minimum
342 values of the aridity index (0.618), and potential evapotranspiration much higher than precipitation.
343 Besides, Ios4 presented a maximum value (0.714) for this region (meaning that water availability in the
344 soil was not compensated by the precipitation of the previous months).

345 Combining all variables, it was possible to distinguish two sub-regions with distinct conditions: the
346 southeast of Alentejo and the Atlantic margin. The latter is mainly composed of podzols and regosols,
347 low slope areas and more humid climatic conditions than the southeast of Alentejo.

348

349 3.3 Regression models



350 The Kernel density of the proxy GDV species, *Q. suber*, *Q. ilex* and *P. pinea*, showed a skewed normal
351 distribution. Therefore, a square-root normalization of the data was applied on this response variable,
352 before model fitting. To be able to compare the resulting model coefficients and use them as weighting
353 factors of the multi-criteria analysis to build the suitability map, the predictor variables were normalized
354 using the z-score function. The equation resulting from the GWR model fitting, featuring the predictor
355 coefficients (Table 2) used later for the computation of the GDV suitability map corresponds to Eq. (4).

356 Local adjusted R-squared was highly variable throughout the study area, ranging from 0.25 to 0.95
357 (fig05). Lower R-squared values were clustered, near the Tagus river basin and in central and northern
358 Alentejo. The overall fit of the GWR model was high (Table 3). The adjusted regression coefficient
359 indicated that 92% of the variation in the data was explained by the GWR model, while only 11% was
360 explained by the simple linear model (Table 3). Accordingly, GWR had a substantially lower AICc when
361 compared with the simple linear model, indicating a much better fit.

362 The analysis of spatial autocorrelation, given by the Moran Index, showed a Z-score of 107.79 for the
363 GWR model, with a considerable reduction of the Moran Index between models, from 0.94 in the simple
364 linear regression model to 0.67 in the GWR model. From figures 06a and 06b there is an evident decrease
365 in clustered residual values from the simple linear model to GWR. In the linear model (fig06a), positive
366 residuals were condensed in the right side of Tagus and Sado river basins, while negative values were
367 mainly present on the left side of the Tagus river and in the center-south of Alentejo. In GWR model
368 (fig06b) the condensed positive and negative residual values were much more scattered throughout the
369 study region, highlighting a much better performance of the GWR, which minimized residual
370 autocorrelation.

371 $Density = 23.88 + 0.22 Ios4 - 1.61 AI + 0.06 Depth + 1.33 Soil\ type\ 2 + 2.46 Soil\ type\ 3 +$
372 $0.14 Slope ,$ (4)

373

374 3.4 GDV Suitability map

375 The classification of the 5 endorsed environmental predictors is presented in Table 4 and their respective
376 maps in figure B1 in appendix. Rivers Tagus and Sado had a positive impact on GDV's suitability to each
377 predictor. This is due to a higher water availability reflected by the values of ombrothermic and aridity
378 indexes (figs. B1a and B1b in appendix) and a higher groundwater depth in the surroundings of the rivers
379 (fig. B1c in appendix). Optimal conditions for groundwater access were mainly gathered in the interior of
380 the study region (fig07), with the exception for some confined aquifers. Favorable slopes for GDV were
381 mostly highlighted in the Tagus river basin area, where a good likelihood of interaction between GDV
382 and groundwater could be identified (fig. B1d in appendix). However, this high likelihood was hindered
383 by the type of soil present in that area (fig. B1e in appendix).

384 The final map illustrating the suitability to GDV is shown in Fig. 7. The largest part of the study area (17
385 538 km²), representing more than half of the total area (55.8%) showed a very good suitability to the
386 occurrence of GDV. The rest of the territory showed a "Moderate" to "Poor" suitability, representing



387 5 037 km² and 4 313 km², respectively. Altogether, 1/3 of the total area showed “Very poor” to
388 “Moderate” suitability to GDV, corresponding to the most southern and eastern part of the study region.

389 The suitability to GDV in the Alentejo region was mainly driven by soil type, given by the similar
390 distribution pattern between the suitability map and the soil type predictor (fig04a and fig07). This was
391 also confirmed by the high coefficient obtained for the soil type predictor in the GWR model equation.
392 The aridity index also showed a strong influence on GDV’s suitability, mostly for the intermediate and
393 good classes. Areas with high suitability classes corresponded to the most northern and coastal areas of
394 Alentejo region. Areas with intermediate class in the north of the study region mostly matched with soil
395 type polygons, with score 1 and 2 (figB1e in appendix), while high aridity values restricted GDV’s
396 suitability in the south. Areas with a good suitability mostly coincided with polygons of soil type 3 and
397 with lower values of aridity index in the northern region of Alentejo.

398

399 3.5 Map validation

400 To assess the quality of the suitability map developed in the present study, we compared our results with
401 integrated suitability maps, from different data sources than those used in this study, for each of the
402 previously considered proxy species. The integrated suitability maps of each proxy species were
403 aggregated into one validation map.

404 Both the result and validation maps were highly coincident, especially with respect to areas with lower
405 and moderate suitability to GDV (Table 5). Areas with very poor GDV suitability corresponded to almost
406 76% of the non-suitable areas for proxy species in the validation map. Accordingly, poor suitability areas
407 for GDV matched 36.65% of the non-suitable areas for proxy species and 45.27% of areas suitable to
408 only one of the proxy species. Besides, areas with moderate GDV suitability matched almost half of the
409 suitable areas for two of the proxy species in the validation map. Classes with higher GDV suitability did
410 not show a good agreement with the validation map.

411 When juxtaposing both maps (fig07 and fig08), there was an overall correspondence between areas with
412 higher suitability to the proxy species. In both maps the northern and coastal area of the Alentejo region,
413 south of the Tagus river basin, showed a matching higher suitability to the proxy species and the GDV.
414 The Sado region was a common area of high suitability in both maps as well. The largest mismatches
415 between maps were found in the center and southeast of the study region.

416 Temporary irrigated areas matched non-suitable areas for proxy species in the validation map (fig C1 in
417 appendix). This could explain some of the mismatches highlighted before, particularly where a large
418 percentage of good and very good GDV suitability (28 and 41% respectively) corresponds to a non-
419 suitable area for each of the proxy species in the validation map (Table5).

420

421



422 **4 Discussion**

423

424 **4.1 Modeling approach**

425 Mapping the suitability of regional Groundwater Dependent Vegetation in southern Portugal proved to be
426 a challenge because of the intricate relations between topographical, hydrological and biotic conditions in
427 this specific area of the Mediterranean basin. Only 50% of the initial predictors were assigned for model
428 fitting, due to a high collinearity between variables of the same type (e.g. aridity index and SPEI
429 variables). Nevertheless, the small number of elected predictors for modeling will provide a higher
430 reliability of the forecast of GDV suitability under future predicted environmental conditions.

431 Despite the exclusion of redundant predictors, the spatial distribution of residues after fitting the simple
432 linear model still showed a significant clustered pattern, which violated the basic assumption of
433 independence between samples. Therefore, a Geographically Weighted Regression model was used
434 according to Stewart Fotheringham et al. (1996). This spatial variation of the linear model has been used
435 before in ecological studies (Li et al., 2016; Mazziotta et al., 2016), but never for the mapping of GDV, to
436 our knowledge. This approach considerably improved the goodness of fit, with a coefficient of regression
437 (R^2) increasing from 0.11 to 0.92 at the global level, and an obvious reduction of residual clustering.
438 Despite those improvements, it has not been possible to completely eliminate the residual autocorrelation
439 after fitting the GWR model.

440 Kernel density for the study area provided a strong indication of presence and abundance of the tree
441 species considered as GDV proxy for modeling. Mediterranean cork woodlands are very particular
442 agroforestry systems present in a confined area of the Mediterranean basin, where sparse tree distributions
443 dominate, because of silvicultural management to increase cork and acorn production, while providing a
444 large grassland area for cattle (Bugalho et al., 2009). However, anthropologic management of
445 agroforestry systems in this region has not been considered in the model. This could, at least partially,
446 explain the non-randomness of the residual distribution after GWR model fitting.

447 Another explanation of the reminiscent autocorrelation after GWR fitting could be the lack of
448 groundwater dependent species in the model. For example, we decided to exclude *Pinus pinaster* Aiton
449 due to its more humid distribution in Portugal, and due to conflicting conclusions driven from previous
450 studies to pin point the species as a potential groundwater use (Bourke, 2004; Kurz-Besson et al., 2016).
451 In addition, only recently the use of groundwater by an olive orchard has been proved (Ferreira et al.,
452 2018), however with little groundwater flow amount of the daily root flow, and so with no significant
453 impact for the species physiological conditions.

454 Methods previously used by Doody et al., (2017) and Condeso de Melo et al. (2015) to map specific
455 vegetation relied solely on expert opinion, e.g. Delphi panel, to define weighting factors of environmental
456 information for GIS multicriteria analysis. In our study, we used GWR to assess weighting factors for
457 each environmental predictor in the study area, to build a suitability map for the GDV in southern



458 Portugal. This allowed an empirical determination of the relevance of each environmental predictor in
459 GDV distribution, thus avoiding the inevitable subjectivity of Delphi panels.

460

461 **4.2 Suitability to Groundwater Dependent Vegetation**

462 As shown by the simulations of future climate conditions based on RCP4.5 and RCP8.5 emission
463 scenarios (Soares et al., 2015, 2017), a significant decrease of precipitation for the Guadiana basin and
464 overall decrease for the southern region of Portugal are expected. Agroforestry systems relying on
465 groundwater resources, such as cork oak woodlands, may show a decrease in productivity and ecosystem
466 services or even face sustainability failure. Therefore, linking s GDV to key environmental drivers and
467 especially climate, will allow to forecast ecological changes under future climatic conditions and spot
468 priority areas for adaptation and stakeholder decision.

469 According to our results, more than half of the study area appears suitable for GDV. However, one third
470 of the studied area showed the lowest suitability to GDV. The lower suitability to this vegetation in the
471 eastern part of the studied area can be explained by less favorable climatic and geological conditions,
472 resulting from the combination of a high aridity index and low water retention at deep soil layers. Soils
473 with lower water capacity further lowered GDV suitability in the most southeastern region of the studied
474 area.

475 An increase in aridity and drought frequency for the Mediterranean (Spinoni et al., 2017) will most
476 probably induce plant physiological adaptations (Peñuelas and Filella, 2001) as well as species
477 substitution (Lloret et al., 2004). In the Mediterranean environment, Peñuelas et al. (2011) distinguished
478 two plant communities regarding water consumption, one with deep roots, able to constantly access water
479 and nutrients and a second community with shallow roots, depending on superficial water from rainfall.
480 Due to climate change conditions, in the Alentejo region of Portugal, we should expect GDV of the less
481 suitable areas to be replaced by the community with shallow roots using rainfall water exclusively. This
482 has already been reported for a Mediterranean woodland of the Iberian Peninsula, where extreme drought
483 conditions led to a shift in vegetation cover from deep-rooting species to water spending species (Caldeira
484 et al., 2015). Groundwater reservoirs would thus no longer be a constraint for plant survival during
485 summer droughts, because the supplanting vegetation community, namely annuals that stop their growing
486 cycle or die before the onset of the dry season, would no longer need constant access to water. Such
487 species substitution would be associated with ecological and biodiversity costs, by shifting from
488 woodland to shrubland ecosystems.

489 In environments with scarce water sources such as the Mediterranean basin, many tree species have
490 adapted to the precipitation's seasonality and its large variability by developing dimorphic root systems.
491 When comparing different water limited ecosystems from a global dataset, Schenk and Jackson (2002)
492 showed that rooting depth increased with aridity. Our results agree with these findings since the aridity
493 index was the second most important predictor of GDV density, according to our equation. Nevertheless,
494 the soil type turned out to be the most important predictor of GDV density. This is comprehensible
495 because the soil type defines the capacity for groundwater storage and the accessibility for deep root



496 system (Centenaro et al., 2017; Grimaldi et al., 2015). However, the soil type component is not expected
497 to change as dramatically as the aridity index in response to climate change, leaving the aridity index as
498 the main driver for the GDV density under climatic changes in southern Portugal.

499 As stated by our model equation, groundwater depth appeared to have little influence on GDV density.
500 This disagrees with our initial hypothesis. However, this disagreement should be regarded cautiously due
501 to the poor quality of the data used. On one hand, data points in the study region were highly
502 heterogeneous, and certain areas showed a better statistical representation than others. Moreover, the high
503 variability in geological media, topography and vegetation cover at the regional scale did not allow to
504 account for small changes in groundwater depth (<15m deep), which has a huge impact on GDV
505 suitability (Canadell et al., 1996; Stone and Kalisz, 1991). Indeed, a high spatial resolution of
506 hydrological database is essential to characterize the spatial dynamics of groundwater depth between
507 hydrographic basins (Lorenzo-Lacruz et al., 2017). However, such resolution was not available for our
508 study area. In addition, the lack of temporal data did not allow the calculation of seasonal trends in
509 groundwater depth, which are essential under Mediterranean conditions to build a reliable interpolation of
510 observed data. Temporal data would also further help discriminate areas of optimal suitability to GDV,
511 either during the wet and the dry seasons.

512 Overall, the map of suitability to GDV showed good results, compared with the validation maps showing
513 the proxy species integrated suitability (Magalhães et al., 2015a, 2015b, 2015c). However, areas of high
514 suitability to GDV matched areas of the validation that were non-suitable areas for the proxy species. This
515 can be explained by the lack of information in the model concerning main land occupation and land
516 management in the studied region. We found that areas where the main land occupation is non-
517 silvicultural (e.g. temporary irrigation fields), corresponded to non-suitable areas for proxy species in the
518 validation map. Several other discrepancies can be explained by additional information considered in the
519 validation map by their authors, such as the current occupation type (e.g. olive orchards, vineyards or
520 urban).

521 The main areas showing good suitability are mostly matching in both maps. Furthermore, our results
522 highly agree with Paulo et al. (2015) who predicted site productivity index and soil variables for cork oak
523 (*Q. suber*) stands in Portugal with a stochastic modelling approach. This allows us to apply the
524 methodology to extend our findings for larger geographical areas such as the Iberian Peninsula. Also, the
525 model equation can be considered reliable to simulate the impact of future climatic conditions on the
526 distribution of GDV in southern Portugal.

527

528 4.3 Key limitations

529 With the methodology applied in this study, weighting factors can be easily evaluated solely from local
530 and regional observations of the studied area. Nonetheless, either the computation of model coefficients
531 or expert opinion to assess weighting factors, require update, and/or environmental data, species
532 distribution and revised expert knowledge (Doody et al., 2017).



533 Changes in climate conditions only represents part of the water resources shortage issue in the future.
534 Global-scale changes in human populations and economic progresses also rules water demand and
535 supply, especially in arid and semi-arid regions (Vörösmarty et al., 2000). A decrease in useful water
536 resources for human supply can induce an even higher pressure on groundwater resources (Döll, 2009),
537 aggravating the water table drawdown caused by climate change (Ertürk et al., 2014). Therefore,
538 additional updates of the model should include human consumption of groundwater resources, identifying
539 areas of higher population density or intensive farming. Future model updates should also account for the
540 interaction of deep rooting species with the surrounding understory species. In particular, shrubs
541 surviving the drought period, which can benefit from the redistribution of groundwater by deep rooted
542 species (Dawson, 1993; Zou et al., 2005).

543

544



545 **5 Conclusions**

546

547 The current pressure applied by human consumption of water sources has reinforced the concern on the
548 future of economic activities dependent on groundwater resources. To address this issue, several countries
549 have developed national strategies for the adaptation of water sources for Agriculture and Forests against
550 Climate Change, including Portugal (FAO, 2007). In addition, local drought management as long-term
551 adaptation strategy has been one of the proposals of Iglesias et al. (2007) to reduce the climate change
552 impact on groundwater resources in the Mediterranean. The preservation of Mediterranean agroforestry
553 systems, such as cork oak woodlands and the recently associated *P. pinea* species, is of great importance
554 due to their high socioeconomic value and their supply of valuable ecosystem services (Bugalho et al.,
555 2011). Management policies on the long-term should account for groundwater resources monitoring,
556 accompanied by defensive measures to ensure agroforestry systems sustainability and economical income
557 from these Mediterranean ecosystems are not greatly and irreversibly threatened.

558 Our present study, and novel methodology, provides an important tool to help delineating priority areas of
559 action for species and groundwater management, at regional level, to avoid the decline of productivity
560 and cover density of the agroforestry systems of southern Portugal. This is important to guarantee the
561 sustainability of the economical income for stakeholders linked to the agroforestry sector in that area.
562 Furthermore, mapping vulnerable areas at a small scale (e.g. by hydrological basin), where reliable
563 groundwater depth information is available, should provide further insights for stakeholder to promote
564 local actions to mitigate climate change impact on GDV.

565 Based on the methodology applied in this work, future predictions on GDV suitability, according to the
566 RCP4.5 and RCP8.5 emission scenarios will be shortly computed, providing guidelines for future
567 management of these ecosystems in the allocation of water resources.

568

569

570

571



572 **6 Acknowledgements**

573

574 The authors acknowledge the E-OBS dataset from the EU-FP6 project ENSEMBLES (<http://ensembles->
575 [eu.metoffice.com](http://metoffice.com)) and the data providers in the ECA&D project (<http://www.ecad.eu>). The authors also
576 wish to acknowledge the ASTER GDEM data product, a courtesy of the NASA Land Processes
577 Distributed Active Archive Center (LP DAAC), USGS/Earth Resources Observation and Science (EROS)
578 Center, Sioux Falls, South Dakota, https://lpdaac.usgs.gov/data_access/data_pool. We are grateful to
579 ICNF for sharing inventory database performed in 2010 in Portugal continental. We also thank Célia
580 Gouveia, Cristina Catita, Ana Russo and Patrícia Páscoa for the advice and helpful comments. We are
581 very grateful to Eric Font for the useful insights on soil properties. I Gomes Marques and research
582 activities were supported by the Portuguese National Foundation for Science and Technology (FCT)
583 through the PIEZAGRO project (PTDC/AAG-REC/7046/2014).

584

585 The authors declare that they have no conflict of interest.

586

587



588 **References**

- 589 Aksoy, E., Louwagie, G., Gardi, C., Gregor, M., Schröder, C. and Löhnertz, M.: Assessing soil
590 biodiversity potentials in Europe, *Sci. Total Environ.*, 589, 236–249, doi:10.1016/j.scitotenv.2017.02.173,
591 2017.
- 592 Anselin, L., Ibnu, S. and Youngihn, K.: GeoDa: An Introduction to Spatial Data Analysis, *Geogr. Anal.*,
593 38(1), 5–22, 2006.
- 594 APA: Plano de Gestão da Região Hidrográfica do Tejo: Parte 2 - Caracterização e Diagnóstico da Região
595 Hidrográfica. [online] Available from:
596 [https://sniambgeoviewer.apambiente.pt/Geodocs/geoportaldocs/Planos/PGRH5-](https://sniambgeoviewer.apambiente.pt/Geodocs/geoportaldocs/Planos/PGRH5-TEJO/RB%5Cpgrhtejo_p2.pdf)
597 [TEJO/RB%5Cpgrhtejo_p2.pdf](https://sniambgeoviewer.apambiente.pt/Geodocs/geoportaldocs/Planos/PGRH5-TEJO/RB%5Cpgrhtejo_p2.pdf) (Accessed 1 February 2018), n.d.
- 598 ARH Alentejo: Plano de Gestão das Bacias Hidrográficas integradas na RH7 - Parte 2. [online] Available
599 from:
600 [https://sniambgeoviewer.apambiente.pt/Geodocs/geoportaldocs/Planos/PGRH7/VolumeI_Relatorio%5C](https://sniambgeoviewer.apambiente.pt/Geodocs/geoportaldocs/Planos/PGRH7/VolumeI_Relatorio%5Cparte2%5CTomo1%5CP2_T1A_RH7_VF.pdf)
601 [arte2%5CTomo1%5CP2_T1A_RH7_VF.pdf](https://sniambgeoviewer.apambiente.pt/Geodocs/geoportaldocs/Planos/PGRH7/VolumeI_Relatorio%5Cparte2%5CTomo1%5CP2_T1A_RH7_VF.pdf) (Accessed 1 February 2018a), 2012.
- 602 ARH Alentejo: Planos de Gestão das Bacias Hidrográficas integradas na RH6 - Parte 2. [online]
603 Available from:
604 [https://sniambgeoviewer.apambiente.pt/Geodocs/geoportaldocs/Planos/PGRH6/VolumeI_Relatorio%5C](https://sniambgeoviewer.apambiente.pt/Geodocs/geoportaldocs/Planos/PGRH6/VolumeI_Relatorio%5Cparte2%5CTomo1%5CP2_T1A_RH6_VF.pdf)
605 [arte2%5CTomo1%5CP2_T1A_RH6_VF.pdf](https://sniambgeoviewer.apambiente.pt/Geodocs/geoportaldocs/Planos/PGRH6/VolumeI_Relatorio%5Cparte2%5CTomo1%5CP2_T1A_RH6_VF.pdf) (Accessed 1 February 2018b), 2012.
- 606 Autoridade Florestal Nacional and Ministério da Agricultura do Desenvolvimento Rural e das Pescas: 5o
607 Inventário Florestal Nacional, 2010.
- 608 Barata, L. T., Saavedra, A., Cortez, N. and Varennes, A.: Cartografia da espessura efectiva dos solos de
609 Portugal Continental. LEAF/ISA/ULisboa. [online] Available from: [http://epic-webgis-](http://epic-webgis-portugal.isa.utl.pt/)
610 [portugal.isa.utl.pt/](http://epic-webgis-portugal.isa.utl.pt/), 2015.
- 611 Barbero, M., Loisel, R. and Quézel, P.: Biogeography, ecology and history of Mediterranean *Quercus ilex*
612 ecosystems, in *Quercus ilex L. ecosystems: function, dynamics and management*, edited by F. Romane
613 and J. Terradas, pp. 19–34, Springer Netherlands, Dordrecht., 1992.
- 614 Barbeta, A. and Peñuelas, J.: Increasing carbon discrimination rates and depth of water uptake favor the
615 growth of Mediterranean evergreen trees in the ecotone with temperate deciduous forests, *Glob. Chang.*
616 *Biol.*, 1–15, doi:10.1111/gcb.13770, 2017.
- 617 Barbeta, A., Mejía-Chang, M., Ogaya, R., Voltas, J., Dawson, T. E. and Peñuelas, J.: The combined
618 effects of a long-term experimental drought and an extreme drought on the use of plant-water sources in a
619 Mediterranean forest, *Glob. Chang. Biol.*, 21(3), 1213–1225, doi:10.1111/gcb.12785, 2015.
- 620 Barron, O. V., Emelyanova, I., Van Niel, T. G., Pollock, D. and Hodgson, G.: Mapping groundwater-
621 dependent ecosystems using remote sensing measures of vegetation and moisture dynamics, *Hydrol.*
622 *Process.*, 28(2), 372–385, doi:10.1002/hyp.9609, 2014.



- 623 Beguería, S. and Vicente-Serrano, S. M.: SPEI: Calculation of the Standardized Precipitation-
624 Evapotranspiration Index. R package version 1.6., 2013.
- 625 Bivand, R. and Yu, D.: spgwr: Geographically Weighted Regression. [online] Available from:
626 <https://cran.r-project.org/package=spgwr>, 2017.
- 627 Bivand, R. S., Pebesma, E. J. and Gómez-Rubio, V.: Applied Spatial Data Analysis with R, edited by G.
628 P. Robert Gentleman, Kurt Hornik, Springer., 2008.
- 629 Bourke, L.: Growth trends and water use efficiency of *Pinus pinaster* Ait. in response to historical climate
630 and groundwater trends on the Gngangara Mound, Western Australia. [online] Available from:
631 http://ro.ecu.edu.au/theses_hons/141 (Accessed 29 January 2018), 2004.
- 632 Bugalho, M. N., Plieninger, T. and Aronson, J.: Open woodlands: a diversity of uses (and overuses), in
633 Cork oak woodlands on the edge, edited by J. Aronson, J. S. Pereira, and J. G. Pausas, pp. 33–48, Island
634 Press, Washington DC., 2009.
- 635 Bugalho, M. N., Caldeira, M. C., Pereira, J. S., Aronson, J. and Pausas, J. G.: Mediterranean cork oak
636 savannas require human use to sustain biodiversity and ecosystem services, *Front. Ecol. Environ.*, 9(5),
637 278–286, doi:10.1890/100084, 2011.
- 638 Bussotti, F., Ferrini, F., Pollastrini, M. and Fini, A.: The challenge of Mediterranean sclerophyllous
639 vegetation under climate change: From acclimation to adaptation, *Environ. Exp. Bot.*, 103(April), 80–98,
640 doi:10.1016/j.envexpbot.2013.09.013, 2013.
- 641 Caldeira, M. C., Lecomte, X., David, T. S., Pinto, J. G., Bugalho, M. N. and Werner, C.: Synergy of
642 extreme drought and shrub invasion reduce ecosystem functioning and resilience in water- limited
643 climates, *Sci. Rep.*, 5(15110), 1-9, doi:10.1038/srep15110, 2015.
- 644 Canadell, J., Jackson, R., Ehleringer, J., Mooney, H. A., Sala, O. E. and Schulze, E.-D.: Maximum
645 rooting depth of vegetation types at the global scale, *Oecologia*, 108, 583–595, doi:10.1007/BF00329030,
646 1996.
- 647 del Castillo, J., Comas, C., Voltas, J. and Ferrio, J. P.: Dynamics of competition over water in a mixed
648 oak-pine Mediterranean forest: Spatio-temporal and physiological components, *For. Ecol. Manage.*, 382,
649 214–224, doi:10.1016/j.foreco.2016.10.025, 2016.
- 650 Centenaro, G., Hudek, C., Zanella, A. and Crivellaro, A.: Root-soil physical and biotic interactions with a
651 focus on tree root systems: A review, *Appl. Soil Ecol.*, doi:10.1016/J.APSOIL.2017.09.017, 2017.
- 652 Chambel, A., Duque, J. and Nascimento, J.: Regional Study of Hard Rock Aquifers in Alentejo, South
653 Portugal: Methodology and Results, in *Groundwater in Fractured Rocks - IAH Selected Paper Series*, pp.
654 73–93, CRC Press., 2007.
- 655 Coelho, I. S. and Campos, P.: Mixed Cork Oak-Stone Pine Woodlands in the Alentejo Region of
656 Portugal, in *Cork Oak Woodlands on the Edge - Ecology, Adaptive Management, and Restoration*, edited
657 by J. Aronson, J. S. Pereira, J. Uli, and G. Pausas, pp. 153–159, Island Press, Washington. [online]



- 658 Available from:
659 <http://citeseerx.ist.psu.edu/viewdoc/download?doi=10.1.1.732.5454&rep=rep1&type=pdf> (Accessed 2
660 February 2018), 2009.
- 661 Condesso de Melo, M. T., Nascimento, J., Silva, A. C., Mendes, M. P., Buxo, A. and Ribeiro, L.:
662 Desenvolvimento de uma metodologia e preparação do respetivo guia metodológico para a identificação e
663 caracterização, a nível nacional, dos ecossistemas terrestres dependentes das águas subterrâneas
664 (ETDAS). Relatório de projeto realizado para a Agência P., 2015.
- 665 Costa, A., Madeira, M. and Oliveira, C.: The relationship between cork oak growth patterns and soil,
666 slope and drainage in a cork oak woodland in Southern Portugal, *For. Ecol. Manage.*, 255, 1525–1535,
667 doi:10.1016/j.foreco.2007.11.008, 2008.
- 668 David, T. S., Ferreira, M. I., Cohen, S., Pereira, J. S. and David, J. S.: Constraints on transpiration from
669 an evergreen oak tree in southern Portugal, *Agric. For. Meteorol.*, 122(3–4), 193–205,
670 doi:10.1016/j.agrformet.2003.09.014, 2004.
- 671 David, T. S., Henriques, M. O., Kurz-Besson, C., Nunes, J., Valente, F., Vaz, M., Pereira, J. S., Siegwolf,
672 R., Chaves, M. M., Gazarini, L. C. and David, J. S.: Water-use strategies in two co-occurring
673 Mediterranean evergreen oaks: surviving the summer drought., *Tree Physiol.*, 27(6), 793–803,
674 doi:10.1093/treephys/27.6.793, 2007.
- 675 David, T. S., Pinto, C. A., Nadezhdina, N., Kurz-Besson, C., Henriques, M. O., Quilhó, T., Cermak, J.,
676 Chaves, M. M., Pereira, J. S. and David, J. S.: Root functioning, tree water use and hydraulic
677 redistribution in *Quercus suber* trees: A modeling approach based on root sap flow, *For. Ecol. Manage.*,
678 307, 136–146, doi:10.1016/j.foreco.2013.07.012, 2013.
- 679 Dawson, T. E.: Hydraulic lift and water use by plants: implications for water balance, performance and
680 plant-plant interactions, *Oecologia*, 95, 565–574 [online] Available from:
681 <https://link.springer.com/content/pdf/10.1007%2FBF00317442.pdf> (Accessed 31 January 2018), 1993.
- 682 Döll, P.: Vulnerability to the impact of climate change on renewable groundwater resources: a global-
683 scale assessment, *Environ. Res. Lett.*, 4(4), 35006–12, doi:10.1088/1748-9326/4/3/035006, 2009.
- 684 Doody, T. M., Barron, O. V., Dowsley, K., Emelyanova, I., Fawcett, J., Overton, I. C., Pritchard, J. L.,
685 Van Dijk, A. I. J. M. and Warren, G.: Continental mapping of groundwater dependent ecosystems: A
686 methodological framework to integrate diverse data and expert opinion, *J. Hydrol. Reg. Stud.*, 10, 61–81,
687 doi:10.1016/j.ejrh.2017.01.003, 2017.
- 688 Dresel, P. E., Clark, R., Cheng, X., Reid, M., Terry, A., Fawcett, J. and Cochrane, D.: Mapping
689 Terrestrial Groundwater Dependent Ecosystems: Method Development and Example Output., 2010.
- 690 Duque-Lazo, J., Navarro-Cerrillo, R. M. and Ruíz-Gómez, F. J.: Assessment of the future stability of cork
691 oak (*Quercus suber* L.) afforestation under climate change scenarios in Southwest Spain, *For. Ecol.*
692 *Manage.*, 409(June 2017), 444–456, doi:10.1016/j.foreco.2017.11.042, 2018.



- 693 Eamus, D., Freund, R., Loomes, R., Hose, G. and Murray, B.: A functional methodology for determining
694 the groundwater regime needed to maintain the health of groundwater-dependent vegetation, *Aust. J.*
695 *Bot.*, 54(2), 97–114, doi:10.1071/BT05031, 2006.
- 696 Eamus, D., Zolfaghar, S., Villalobos-Vega, R., Cleverly, J. and Huete, A.: Groundwater-dependent
697 ecosystems: Recent insights from satellite and field-based studies, *Hydrol. Earth Syst. Sci.*, 19(10), 4229–
698 4256, doi:10.5194/hess-19-4229-2015, 2015.
- 699 Ertürk, A., Ekdal, A., Gürel, M., Karakaya, N., Guzel, C. and Gönenç, E.: Evaluating the impact of
700 climate change on groundwater resources in a small Mediterranean watershed, *Sci. Total Environ.*, 499,
701 437–447, doi:10.1016/j.scitotenv.2014.07.001, 2014.
- 702 Evaristo, J. and McDonnell, J. J.: Prevalence and magnitude of groundwater use by vegetation: a global
703 stable isotope meta-analysis, *Sci. Rep.*, 7, 44110, doi:10.1038/srep44110, 2017.
- 704 FAO: Adaptation to climate change in agriculture, forestry and fisheries: Perspective, framework and
705 priorities, Rome. [online] Available from:
706 http://www.fao.org/nr/climpag/pub/adaptation_to_climate_change_2007.pdf (Accessed 31 January 2018),
707 2007.
- 708 FAO, IIASA, ISRIC, ISS-CAS and JRC: Harmonized World Soil Database (version 1.1), 2009.
- 709 Fernandes, N. P.: Ecosistemas Dependentes de Água Subterrânea no Algarve - Contributo para a sua
710 Identificação e Caracterização, University of Algarve., 2013.
- 711 Ferreira, M. I., Green, S., Conceição, N. and Fernández, J.-E.: Assessing hydraulic redistribution with the
712 compensated average gradient heat-pulse method on rain-fed olive trees, *Plant Soil*, 1–21,
713 doi:10.1007/s11104-018-3585-x, 2018.
- 714 Filella, I. and Peñuelas, J.: Indications of hydraulic lift by *Pinus halepensis* and its effects on the water
715 relations of neighbour shrubs, *Biol. Plant.*, 47(2), 209–214, doi:10.1023/B:BIOP.0000022253.08474.fd,
716 2004.
- 717 Giorgi, F. and Lionello, P.: Climate change projections for the Mediterranean region, *Glob. Planet.*
718 *Change*, 63(2–3), 90–104, doi:10.1016/j.gloplacha.2007.09.005, 2008.
- 719 Grimaldi, S., Orellana, F. and Daly, E.: Modelling the effects of soil type and root distribution on shallow
720 groundwater resources, *Hydrol. Process.*, 29(20), 4457–4469, doi:10.1002/hyp.10503, 2015.
- 721 Grossiord, C., Sevanto, S., Dawson, T. E., Adams, H. D., Collins, A. D., Dickman, L. T., Newman, B. D.,
722 Stockton, E. A. and McDowell, N. G.: Warming combined with more extreme precipitation regimes
723 modifies the water sources used by trees, *New Phytol.*, doi:10.1111/nph.14192, 2016.
- 724 Guisan, A. and Thuiller, W.: Predicting species distribution: Offering more than simple habitat models,
725 *Ecol. Lett.*, 8(9), 993–1009, doi:10.1111/j.1461-0248.2005.00792.x, 2005.



- 726 Haylock, M. R., Hofstra, N., Klein Tank, A. M. G., Klok, E. J., Jones, P. D. and New, M.: A European
727 daily high-resolution gridded data set of surface temperature and precipitation for 1950-2006, *J. Geophys.*
728 *Res. Atmos.*, 113(20), doi:10.1029/2008JD010201, 2008.
- 729 Hernández-Santana, V., David, T. S. and Martínez-Fernández, J.: Environmental and plant-based
730 controls of water use in a Mediterranean oak stand, *For. Ecol. Manage.*, 255, 3707–3715,
731 doi:10.1016/j.foreco.2008.03.004, 2008.
- 732 Horton, J. L. and Hart, S. C.: Hydraulic lift: a potentially important ecosystem process, *Tree*, 13(6), 232–
733 235, doi:10.1016/j.tree.1998.03.004, 1998.
- 734 Howard, J. and Merrifield, M.: Mapping groundwater dependent ecosystems in California, *PLoS One*,
735 5(6), doi:10.1371/journal.pone.0011249, 2010.
- 736 Hu, X., Zhang, L., Ye, L., Lin, Y. and Qiu, R.: Locating spatial variation in the association between road
737 network and forest biomass carbon accumulation, *Ecol. Indic.*, 73, 214–223,
738 doi:10.1016/j.ecolind.2016.09.042, 2017.
- 739 ICNF: IFN6 – Áreas dos usos do solo e das espécies florestais de Portugal continental. Resultados
740 preliminares., Lisboa. [online] Available from:
741 <http://www2.icnf.pt/portal/florestas/ifn/resource/ficheiros/ifn/ifn6-res-prelimv1-1> (Accessed 9 January
742 2018), 2013.
- 743 Iglesias, A., Garrote, L., Flores, F. and Moneo, M.: Challenges to manage the risk of water scarcity and
744 climate change in the Mediterranean, *Water Resour. Manag.*, 21, 775–788, doi:10.1007/s11269-006-
745 9111-6, 2007.
- 746 Joffre, R., Rambal, S. and Ratte, J. P.: The dehesa system of southern Spain and Portugal as a natural
747 ecosystem mimic, *Agrofor. Syst.*, 45, 57–79, doi:10.1023/a:1006259402496, 1999.
- 748 Kurz-Besson, C., Otieno, D., Lobo Do Vale, R., Siegwolf, R., Schmidt, M., Herd, A., Nogueira, C.,
749 David, T. S., David, J. S., Tenhunen, J., Pereira, J. S. and Chaves, M.: Hydraulic lift in cork oak trees in a
750 savannah-type Mediterranean ecosystem and its contribution to the local water balance, *Plant Soil*, 282(1–
751 2), 361–378, doi:10.1007/s11104-006-0005-4, 2006.
- 752 Kurz-Besson, C., Lobo-do-Vale, R., Rodrigues, M. L., Almeida, P., Herd, A., Grant, O. M., David, T. S.,
753 Schmidt, M., Otieno, D., Keenan, T. F., Gouveia, C., Mériaux, C., Chaves, M. M. and Pereira, J. S.:
754 Cork oak physiological responses to manipulated water availability in a Mediterranean woodland, *Agric.*
755 *For. Meteorol.*, 184(December 2013), 230–242, doi:10.1016/j.agrformet.2013.10.004, 2014.
- 756 Kurz-Besson, C., Lousada, J. L., Gaspar, M. J., Correia, I. E., David, T. S., Soares, P. M. M., Cardoso, R.
757 M., Russo, A., Varino, F., Mériaux, C., Trigo, R. M. and Gouveia, C. M.: Effects of recent minimum
758 temperature and water deficit increases on *Pinus pinaster* radial growth and wood density in southern
759 Portugal, *Front. Plant Sci*, 7, doi:10.3389/fpls.2016.01170, 2016.



- 760 Li, Y., Jiao, Y. and Browder, J. A.: Modeling spatially-varying ecological relationships using
761 geographically weighted generalized linear model: A simulation study based on longline seabird bycatch,
762 *Fish. Res.*, 181, 14–24, doi:10.1016/j.fishres.2016.03.024, 2016.
- 763 Lloret, F., Siscart, D. and Dalmases, C.: Canopy recovery after drought dieback in holm-oak
764 Mediterranean forests of Catalonia (NE Spain), *Glob. Chang. Biol.*, 10(12), 2092–2099,
765 doi:10.1111/j.1365-2486.2004.00870.x, 2004.
- 766 López, B., Sabaté, S., Ruiz, I. and Gracia, C.: Effects of Elevated CO₂ and Decreased Water Availability
767 on Holm-Oak Seedlings in Controlled Environment Chambers, in *Impacts of Global Change on Tree
768 Physiology and Forest Ecosystems: Proceedings of the International Conference on Impacts of Global
769 Change on Tree Physiology and Forest Ecosystems*, held 26–29 November 1996, Wageningen, The
770 Netherlands, edited by G. M. J. Mohren, K. Kramer, and S. Sabaté, pp. 125–133, Springer Netherlands,
771 Dordrecht., 1997.
- 772 Lorenzo-Lacruz, J., Garcia, C. and Morán-Tejeda, E.: Groundwater level responses to precipitation
773 variability in Mediterranean insular aquifers, *J. Hydrol.*, 552, 516–531, doi:10.1016/j.jhydrol.2017.07.011,
774 2017.
- 775 Lowry, C. S. and Loheide, S. P.: Groundwater-dependent vegetation: Quantifying the groundwater
776 subsidy, *Water Resour. Res.*, 46(6), doi:10.1029/2009WR008874, 2010.
- 777 Lv, J., Wang, X. S., Zhou, Y., Qian, K., Wan, L., Eamus, D. and Tao, Z.: Groundwater-dependent
778 distribution of vegetation in Hailiutu River catchment, a semi-arid region in China, *Ecohydrology*, 6(1),
779 142–149, doi:10.1002/eco.1254, 2013.
- 780 Magalhães, M. R., Müller, A. and Ferreira Silva, J.: Aptidão Integrada à Azinheira (*Quercus rotundifolia*)
781 para Portugal Continental. LEAF/ISA/ULisboa., [online] Available from: [http://epic-webgis-
782 portugal.isa.utl.pt/](http://epic-webgis-portugal.isa.utl.pt/), 2015a.
- 783 Magalhães, M. R., Müller, A. and Ferreira Silva, J.: Aptidão Integrada ao Pinheiro-manso (*Pinus Pinea*
784 L.) para Portugal Continental. LEAF/ISA/ULisboa., [online] Available from: [http://epic-webgis-
785 portugal.isa.utl.pt/](http://epic-webgis-portugal.isa.utl.pt/), 2015b.
- 786 Magalhães, M. R., Müller, A. and Ferreira Silva, J.: Aptidão Integrada ao Sobreiro (*Quercus suber* L.)
787 para Portugal Continental. LEAF/ISA/ULisboa., [online] Available from: [http://epic-webgis-
788 portugal.isa.utl.pt/](http://epic-webgis-portugal.isa.utl.pt/), 2015c.
- 789 Mazziotta, A., Heilmann-Clausen, J., Bruun, H. H., Fritz, Ö., Aude, E. and Tøttrup, A. P.: Restoring
790 hydrology and old-growth structures in a former production forest: Modelling the long-term effects on
791 biodiversity, *For. Ecol. Manage.*, 381, 125–133, doi:10.1016/j.foreco.2016.09.028, 2016.
- 792 McKee, T. B., Doesken, N. J. and Kleist, J.: The relationship of drought frequency and duration to time
793 scales, in *AMS 8th Conference on Applied Climatology*, pp. 179–184., 1993.



- 794 Mendes, M. P., Ribeiro, L., David, T. S. and Costa, A.: How dependent are cork oak (*Quercus suber* L.)
795 woodlands on groundwater? A case study in southwestern Portugal, *For. Ecol. Manage.*, 378, 122–130,
796 doi:10.1016/j.foreco.2016.07.024, 2016.
- 797 Middleton, N., Thomas, D. S. G. and Programme., U. N. E.: World atlas of desertification, UNEP, 1992.,
798 London., 1992.
- 799 Miller, G. R., Chen, X., Rubin, Y., Ma, S. and Baldocchi, D. D.: Groundwater uptake by woody
800 vegetation in a semiarid oak savanna, *Water Resour. Res.*, 46(10), doi:10.1029/2009WR008902, 2010.
- 801 Ministério da Agricultura do Mar do Ambiente e do Ordenamento do Território: Estratégia de Adaptação
802 da Agricultura e das Florestas às Alterações Climáticas, Lisbon, 2013.
- 803 Montero, G., Ruiz-Peinado, R., Candela, J. A., Canellas, I., Gutierrez, M., Pavon, J., Alonso, A., Rio, M.
804 d., Bachiller, A. and Calama, R.: El pino pinonero (*Pinus pinea* L.) en Andalucía. Ecología, distribución y
805 selvicultura, edited by G. Montero, J. A. Candela, and A. Rodriguez, Consejería de Medio Ambiente,
806 Junta de Andalucía, Sevilla., 2004.
- 807 Moran, P. A. P.: Notes on continuous stochastic phenomena, *Biometrika*, 37(1–2), 17–23 [online]
808 Available from: <http://dx.doi.org/10.1093/biomet/37.1-2.17>, 1950.
- 809 Mourato, S., Moreira, M. and Corte-Real, J.: Water resources impact assessment under climate change
810 scenarios in Mediterranean watersheds, *Water Resour. Manag.*, 29(7), 2377–2391, doi:10.1007/s11269-
811 015-0947-5, 2015.
- 812 Münch, Z. and Conrad, J.: Remote sensing and GIS based determination of groundwater dependent
813 ecosystems in the Western Cape, South Africa, *Hydrogeol. J.*, 15(1), 19–28, doi:10.1007/s10040-006-
814 0125-1, 2007.
- 815 Nadezhkina, N., Ferreira, M. I., Conceição, N., Pacheco, C. A., Häusler, M. and David, T. S.: Water
816 uptake and hydraulic redistribution under a seasonal climate: Long-term study in a rainfed olive orchard,
817 *Ecohydrology*, 8(3), 387–397, doi:10.1002/eco.1545, 2015.
- 818 Neumann, R. B. and Cardon, Z. G.: The magnitude of hydraulic redistribution by plant roots: a review
819 and synthesis of empirical and modeling studies, *New Phytol.*, 194(2), 337–352, doi:10.1111/j.1469-
820 8137.2012.04088.x, 2012.
- 821 O’Grady, A. P., Eamus, D., Cook, P. G. and Lamontagne, S.: Groundwater use by riparian vegetation in
822 the wet–dry tropics of northern Australia, *Aust. J. Bot.*, 54, 145–154, doi:10.1071/BT04164, 2006.
- 823 Orellana, F., Verma, P., Loheide, S. P. and Daly, E.: Monitoring and modeling water-vegetation
824 interactions in groundwater-dependent ecosystems, *Rev. Geophys.*, 50(3), doi:10.1029/2011RG000383,
825 2012.
- 826 Otieno, D. O., Kurz-Besson, C., Liu, J., Schmidt, M. W. T., Do, R. V. L., David, T. S., Siegwolf, R.,
827 Pereira, J. S. and Tenhunen, J. D.: Seasonal variations in soil and plant water status in a *Quercus suber* L.



- 828 stand: Roots as determinants of tree productivity and survival in the Mediterranean-type ecosystem, *Plant*
829 *Soil*, 283(1–2), 119–135, doi:10.1007/s11104-004-7539-0, 2006.
- 830 Paulo, J. A., Palma, J. H. N., Gomes, A. A., Faias, S. P., Tomé, J. and Tomé, M.: Predicting site index
831 from climate and soil variables for cork oak (*Quercus suber* L.) stands in Portugal, *New For.*, 46, 293–
832 307, doi:10.1007/s11056-014-9462-4, 2015.
- 833 Peñuelas, J. and Filella, I.: Responses to a Warming World, *Science*. 294(5543), 793–795,
834 doi:10.1126/science.1066860, 2001.
- 835 Peñuelas, J. and Filella, I.: Deuterium labelling of roots provides evidence of deep water access and
836 hydraulic lift by *Pinus nigra* in a Mediterranean forest of NE Spain, *Environ. Exp. Bot.*, 49(3), 201–208,
837 doi:10.1016/S0098-8472(02)00070-9, 2003.
- 838 Peñuelas, J., Terradas, J. and Lloret, F.: Solving the conundrum of plant species coexistence: Water in
839 space and time matters most, *New Phytol.*, 189(1), 5–8, doi:10.1111/j.1469-8137.2010.03570.x, 2011.
- 840 Pérez Hoyos, I., Krakauer, N., Khanbilvardi, R. and Armstrong, R.: A Review of advances in the
841 identification and characterization of groundwater dependent ecosystems using geospatial technologies,
842 *Geosciences*, 6(2), 17, doi:10.3390/geosciences6020017, 2016a.
- 843 Pérez Hoyos, I., Krakauer, N. and Khanbilvardi, R.: Estimating the probability of vegetation to be
844 groundwater dependent based on the evaluation of tree models, *Environments*, 3(2), 9,
845 doi:10.3390/environments3020009, 2016b.
- 846 Pinto-Correia, T., Ribeiro, N. and Sá-Sousa, P.: Introducing the montado, the cork and holm oak
847 agroforestry system of Southern Portugal, *Agrofor. Syst.*, 82(2), 99–104, doi:10.1007/s10457-011-9388-
848 1, 2011.
- 849 QGIS Development Team: QGIS Geographic Information System. Open Source Geospatial Foundation
850 Project., 2017.
- 851 R Development Core Team: R: A language and environment for statistical computing. R Foundation for
852 Statistical Computing, Vienna, Austria, 2016.
- 853 Rivas-Martínez, S., Rivas-Sáenz, S. and Penas-Merino, A.: Worldwide bioclimatic classification system,
854 *Glob. Geobot.*, 1(1), 1–638, doi:10.5616/gg110001, 2011.
- 855 Robinson, T. W.: Phreatophytes, *United States Geol. Surv. Water-Supply Pap.*, (1423), 84, 1958.
- 856 Sabaté, S., Gracia, C. A. and Sánchez, A.: Likely effects of climate change on growth of *Quercus ilex*,
857 *Pinus halepensis*, *Pinus pinaster*, *Pinus sylvestris* and *Fagus sylvatica* forests in the Mediterranean region,
858 *For. Ecol. Manage.*, 162(1), 23–37, doi:10.1016/S0378-1127(02)00048-8, 2002.
- 859 Sardans, J. and Peñuelas, J.: Increasing drought decreases phosphorus availability in an evergreen
860 Mediterranean forest, *Plant Soil*, 267(1–2), 367–377, doi:10.1007/s11104-005-0172-8, 2004.



- 861 Sarmento, E. de M. and Dores, V.: The performance of the forestry sector and its relevance for the
862 portuguese economy, *Rev. Port. Estud. Reg.*, 34(3), 35–50 [online] Available from:
863 <http://www.apdr.pt/siterper/numeros/RPER34/34.4.pdf> (Accessed 16 February 2018), 2013.
- 864 Schenk, H. J. and Jackson, R. B.: Rooting depths, lateral root spreads and belowground aboveground
865 allometries of plants in water limited ecosystems, *J. Ecol.*, 480–494, doi:10.1046/j.1365-
866 2745.2002.00682.x, 2002.
- 867 Soares, P. M. M., Cardoso, R. M., Ferreira, J. J. and Miranda, P. M. A.: Climate change and the
868 Portuguese precipitation: ENSEMBLES regional climate models results, *Clim. Dyn.*, 45(7–8), 1771–
869 1787, doi:10.1007/s00382-014-2432-x, 2015.
- 870 Soares, P. M. M., Cardoso, R. M., Lima, D. C. A. and Miranda, P. M. A.: Future precipitation in Portugal:
871 high-resolution projections using WRF model and EURO-CORDEX multi-model ensembles, *Clim Dyn.*,
872 49, 2503–2530, doi:10.1007/s00382-016-3455-2, 2017.
- 873 Spinoni, J., Vogt, J. V., Naumann, G., Barbosa, P. and Dosio, A.: Will drought events become more
874 frequent and severe in Europe?, *Int. J. Climatol.*, 38(4), 1718–1736, doi:10.1002/joc.5291, 2017.
- 875 Stewart Fotheringham, A., Charlton, M. and Brunson, C.: The geography of parameter space: an
876 investigation of spatial non-stationarity, *Int. J. Geogr. Inf. Syst.*, 10(5), 605–627,
877 doi:10.1080/02693799608902100, 1996.
- 878 Stone, E. L. and Kalisz, P. J.: On the maximum extent of tree roots, *For. Ecol. Manage.*, 46(1–2), 59–102,
879 doi:10.1016/0378-1127(91)90245-Q, 1991.
- 880 Thornthwaite, C. W.: An approach toward a rational classification of climate, *Geogr. Rev.*, 38(1), 55–94,
881 1948.
- 882 Valentini, R., Scarascia, G. E. and Ehleringer, J. R.: Hydrogen and carbon isotope ratios of selected
883 species of a Mediterranean macchia ecosystem, *Funct. Ecol.*, 6(6), 627–631, 1992.
- 884 Vicente-Serrano, S. M., Beguería, S. and López-Moreno, J. I.: A multiscalar drought index sensitive to
885 global warming: The standardized precipitation evapotranspiration index, *J. Clim.*, 23(7), 1696–1718,
886 doi:10.1175/2009JCLI2909.1, 2010.
- 887 Vörösmarty, C. J., Green, P., Salisbury, J. and Lammers, R. B.: Global water resources: Vulnerability
888 from climate change and population growth, *Science (80-.)*, 289, 284–288,
889 doi:10.1126/science.289.5477.284, 2000.
- 890 Zou, C. B., Barnes, P. W., Archer, S. and Mcmurtry, C. R.: Soil moisture redistribution as a mechanism
891 of facilitation in savanna tree–shrub clusters, *Ecophysiology*, (145), 32–40, doi:10.1007/s00442-005-
892 0110-8, 2005.
- 893
- 894



895 **Figure and Table Legends**

896

897 Table 1: Environmental variables for the study area characterization in suitability to Groundwater Dependent
898 Vegetation.

899 Table 2: Coefficients of determination resulting from the application of GWR model between GDV density and the
900 selected predictive variables.

901 Table 3: Comparison of Adjusted R-squared and second-order Akaike Information Criterion (AICc) between simple
902 regression and GWR models.

903 Table 4: Classification scores for each predictor. A score of 1 was given to areas less suitable and 3 to highly suitable
904 areas.

905 Table 5: Interception (in %) between the classes of the GDV suitability map classes and the Overlapped Integrated
906 suitability map. Value of “0” in overlapped integrated suitability map represent the non-suitable area for all the proxy
907 species; value of “1” represent the suitable area for 1 of the proxy species; value of “2” represent the suitable area for
908 2 of the proxy species and value of “3” represent the suitable area for all the proxy species.

909 Table A1: Squared correlations between predictor variables and principal components axis. The most important
910 predictors for each axis (when squared correlation is above 0.3) are showed in bold.

911

912 Figure 01: Study area. On the left the location of Alentejo in the Iberian Peninsula; on the right, the elevation
913 characterization of the study area with the main river courses from Tagus, Sado and Guadiana basins. Names of the
914 main rivers are indicated near to their location in the map.

915 Figure 02: Large well and piezometer data points used for Water Table Depth calculation. Squares represent
916 piezometers data points and triangle represent large well data points.

917 Figure 03: Map of Kernel Density weighted by cover percentage of *Q. suber*, *Q. ilex* and *P. pinea*.

918 Figure 04: Map of environmental layers used in model fitting. (a) – Soil type; (b) – Slope; (c) – Groundwater Depth
919 (Depth); (d) – Ombrothermic Index of the summer quarter and the immediately previous month (Ios4); (e) – Aridity
920 Index (AI).

921 Figure 05: Spatial distribution of local R^2 from the fitting of the Geographically Weighted Regression.

922 Figure 06: Spatial distribution of residuals from the fitting of the Simple Linear model (a) and Geographically Weighted
923 Regression (b).

924 Figure 07: Suitability map for Groundwater Dependent Vegetation.

925 Figure 08: Validation map corresponding to the juxtaposition of the integrated suitability maps for each of the proxy
926 species *Q. suber*, *Q. ilex* and *P. pinea*. Areas suitable for more than 1 or more proxy species are represented with a
927 gradient of brown colors. Rivers and dams are indicated in blue and artificialized areas in grey.

928 Figure A2: Correlation plot between predictors used for fitting the simple linear model and the GWR model. AI is
929 Aridity Index; Depth is Groundwater Depth (Depth) and Ios4 is the Ombrothermic Index of the summer quarter and
930 the immediately previous month.



931 Figure B1 – Predictors maps after classification. (a) – Ombrothermic Index of the summer quarter and the
932 immediately previous month (Ios4); (b) – Aridity Index (AI); (c) – Groundwater Depth (Depth); (d) – Slope; (e) –
933 Soil type.
934
935



936 **Table 1: Environmental variables for the study area characterization in suitability to Groundwater Dependent**
 937 **Vegetation.**

Variable code	Variable type	Source	Resolution and Spatial extent
Slope	Slope (%)	This work	0.000256 degrees (25m) raster resolution
Soil type	Soil type in the first soil layer	SNIAmb (© Agência Portuguesa do Ambiente, I.P., 2017)	Converted from vectorial to 0.000256 degrees (25m) resolution raster
Thickness	Soil thickness (cm)	EPIC WebGIS Portugal (Barata et al., 2015)	Converted from vectorial to 0.000256 degrees (25m) resolution raster
Depth	Depth to groundwater (m)	This work	0.000256 degrees (25m) raster resolution
Dd	Drainage Density	This work	0.000256 degrees (25m) raster resolution
Spei_severe	Number of months with severe SPEI	This work	0.000256 degrees (25m) raster resolution Time coverage 1950-2010
SPEI_extreme	Number of months with extreme SPEI	This work	0.000256 degrees (25m) raster resolution Time coverage 1950-2010
AI	Aridity Index	This work	0.000256 degrees (25m) raster resolution Time coverage 1950-2010
Io	Annual Ombrothermic Index Annual average (January to December)	This work	0.000256 degrees (25m) raster resolution Time coverage 1950-2010
Ios1	Ombrothermic Index of the hottest month of the summer quarter (J, J and A)	This work	0.000256 degrees (25m) raster resolution Time coverage 1950-2010
Ios3	Ombrothermic Index of the summer quarter (J, J and A)	This work	0.000256 degrees (25m) raster resolution Time coverage 1950-2010
Ios4	Ombrothermic Index of the summer quarter and the immediately previous month (M, J, J and A)	This work	0.000256 degrees (25m) raster resolution Time coverage 1950-2010

938

939

940

941

942

943

944

945



946

947 **Table 2: Coefficients of determination resulting from the application of GWR model between GDV density**
 948 **and the selected predictive variables.**

Variables	Minimum	1 st Quartile	Median	3 rd Quartile	Maximum	Global
Intercept	-48.55	16.01	23.88	29.16	94.65	13.86
Ios4	-18.31	-2.47	0.22	3.13	16.29	-0.22
AI	-48.27	-11.22	-1.61	5.48	64.87	-0.72
Depth	-32.30	-1.08	0.06	0.95	33.25	0.43
Soil type (2)	-19.78	-1.34	1.33	3.97	24.32	3.98
Soil type (3)	-20.18	-0.48	2.46	5.13	23.17	7.62
Slope	-2.88	-0.18	0.14	0.68	4.75	-0.13

949

950 **Table 3: Comparison of Adjusted R-squared and second-order Akaike Information Criterion (AICc) between**
 951 **simple regression and GWR models.**

Model	R-squared	AICc	p-value
OLS	0.11	42276	<0.001
GWR	0.92 *	27795	-

952 *Quasi-global R²

953

954

955 **Table 4: Classification scores for each predictor. A score of 1 was given to areas less suitable and 3 to highly**
 956 **suitable areas.**

Predictor	Class	Score
Slope	0%-5%	3
	5%-10%	2
	>10%	1
Soil type	Eutric Cambisols; Dystric Regosol; Humic Cambisols; Haplic Luvisols; Gleyic Luvisols; Ferric Luvisols; Chromic Luvisols associated with Haplic Luvisols; Ortic Podzols	3
	Calcaric Cambisols; Dystric Regosol associated with Umbric Leptosols; Eutric Regosols; Vertic Luvisols; Eutric Planosols; Cambic Arenosols	2
	Chromic Cambisols; Eutric fluvisols; Chromic Luvisols; Gleyic Solonchak; Eutric Vertisols	1
Groundwater Depth	>15 m	1
	1.5m-15m	3
	≤1.5m	1
Aridity Index	0.6-0.68	3
	0.68-0.75	2
	≥0.75	1
Ios4	<0.28	3
	0.28-0.64	2
	≥0.64	1

957

958

959

960



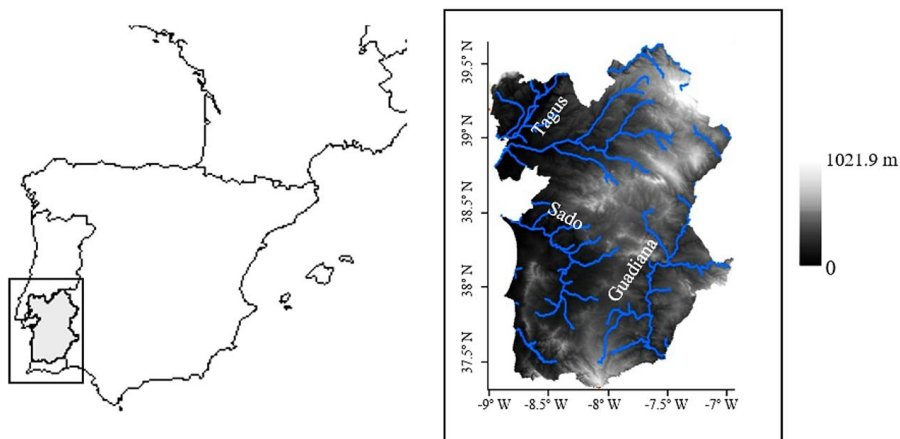
961

962

963 **Table 5: Interception (in %) between the classes of the GDV suitability map classes and the Overlapped**
 964 **Integrated suitability map. Value of “0” in overlapped integrated suitability map represent the non-suitable area**
 965 **for all the proxy species; value of “1” represent the suitable area for 1 of the proxy species; value of “2” represent**
 966 **the suitable area for 2 of the proxy species and value of “3” represent the suitable area for all the proxy species.**

967

GDV suitability	Validation map (Integrated Suitability for 0 to 3 of the proxy species)	% 968
Very Poor	0	75.67
	1	19.78
	2	2.8
	3	0.23
Poor	0	36.65
	1	45.27
	2	14.90
	3	0.02
Moderate	0	33.17
	1	15.53
	2	49.15
	3	0.03
Good	0	38.38
	1	29.51
	2	30.48
	3	0.15
Very Good	0	41.124
	1	18.38
	2	37.81
	3	0.57

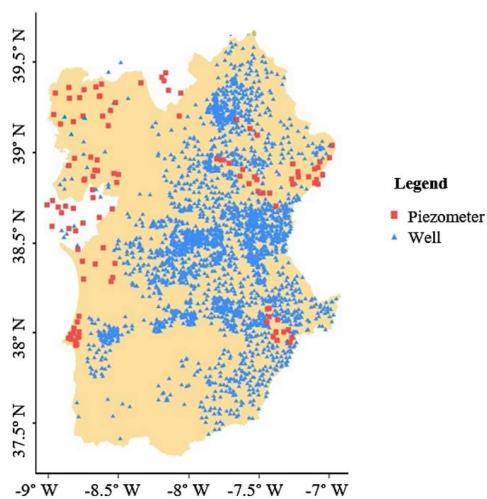


969

970

971 **Figure 01: Study area. On the left the location of Alentejo in the Iberian Peninsula; on the right, the elevation**
972 **characterization of the study area with the main river courses from Tagus, Sado and Guadiana basins. Names**
973 **of the main rivers are indicated near to their location in the map.**

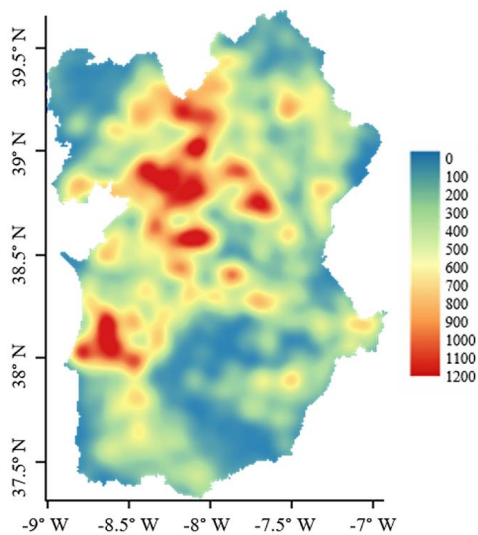
974



975

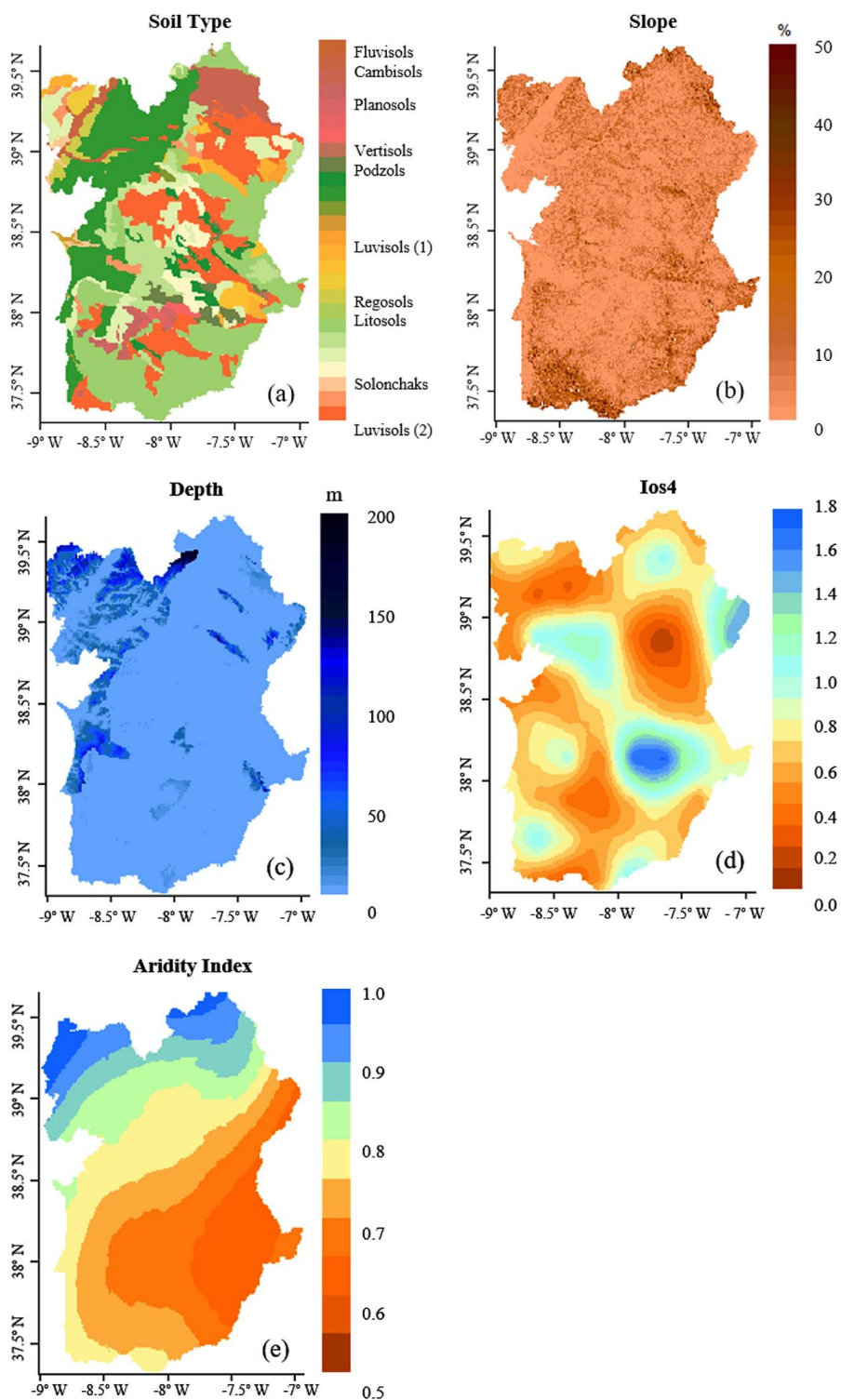
976 **Figure 02: Large well and piezometer data points used for Water Table Depth calculation. Squares represent**
977 **piezometers data points and triangle represent large well data points.**

978



979

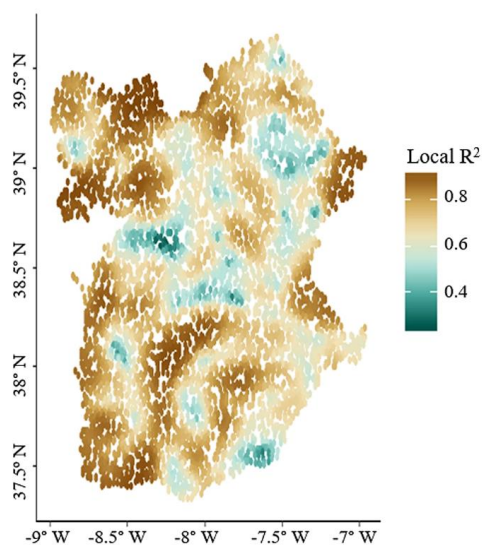
980 **Figure 03: Map of Kernel Density weighted by cover percentage of *Q. suber*, *Q. ilex* and *P. pinea*.**





982 **Figure 04: Map of environmental layers used in model fitting. (a) – Soil type; (b) – Slope; (c) – Groundwater**
983 **Depth (Depth); (d) – Ombrothermic Index of the summer quarter and the immediately previous month (Ios4);**
984 **(e) – Aridity Index (AI).**

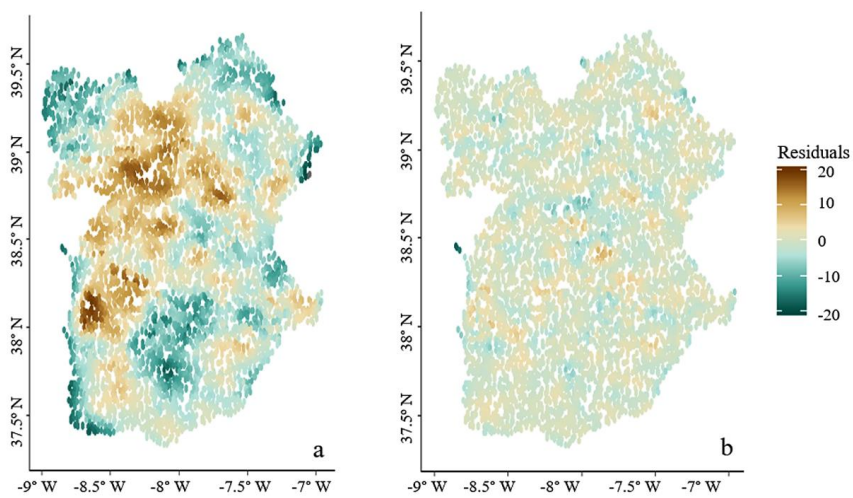
985



986

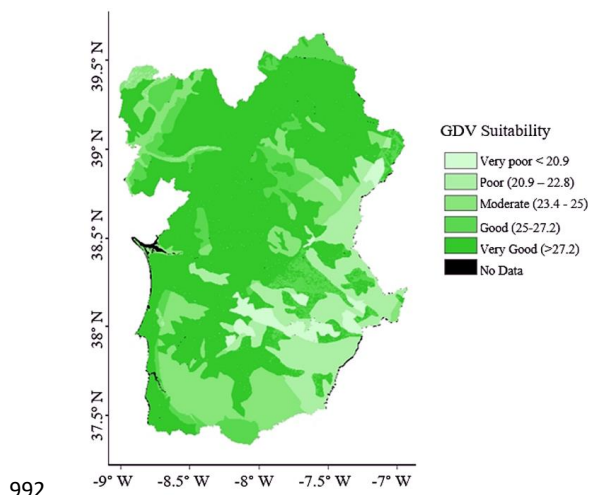
987 **Figure 05: Spatial distribution of local R^2 from the fitting of the Geographically Weighted Regression.**

988



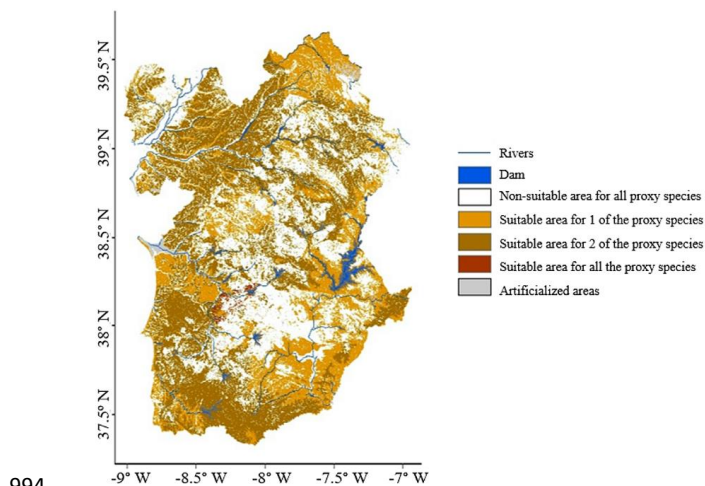
989

990 **Figure 06: Spatial distribution of residuals from the fitting of the Simple Linear model (a) and Geographically**
991 **Weighted Regression (b).**



992

993 **Figure 07: Suitability map for Groundwater Dependent Vegetation.**



994

995 **Figure 08: Validation map corresponding to the juxtaposition of the integrated suitability maps for each of the**
 996 **proxy species *Q. suber*, *Q. ilex* and *P. pinea*. Areas suitable for more than 1 or more proxy species are represented**
 997 **with a gradient of brown colors. Rivers and dams are indicated in blue and artificialized areas in grey.**

998

999



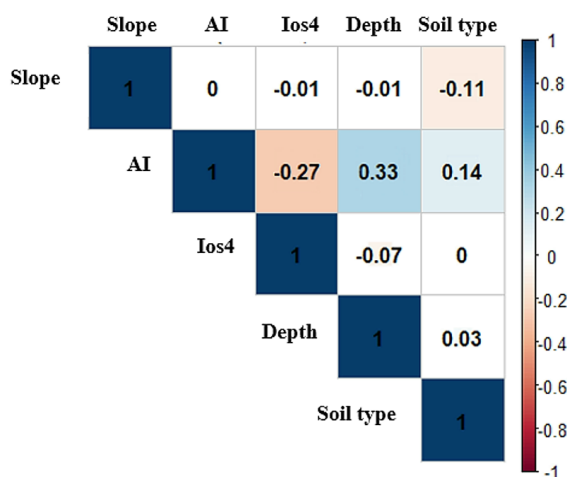
1000 **Appendix A**

1001

1002 **Table A1: Squared correlations between predictor variables and principal components axis. The most**
 1003 **important predictors for each axis (when squared correlation is above 0.3) are showed in bold.**

	PC1	PC2	PC3	PC4	PC5
Slope	<0.01	0.34	0.63	0.03	<0.01
AI	0.67	0.02	<0.001	<0.01	0.31
Ios4	0.18	0.45	0.24	0.03	0.10
Depth	0.43	<0.01	0.06	0.45	0.06
Soil type	0.33	0.25	0.05	0.29	0.08

1004



1005

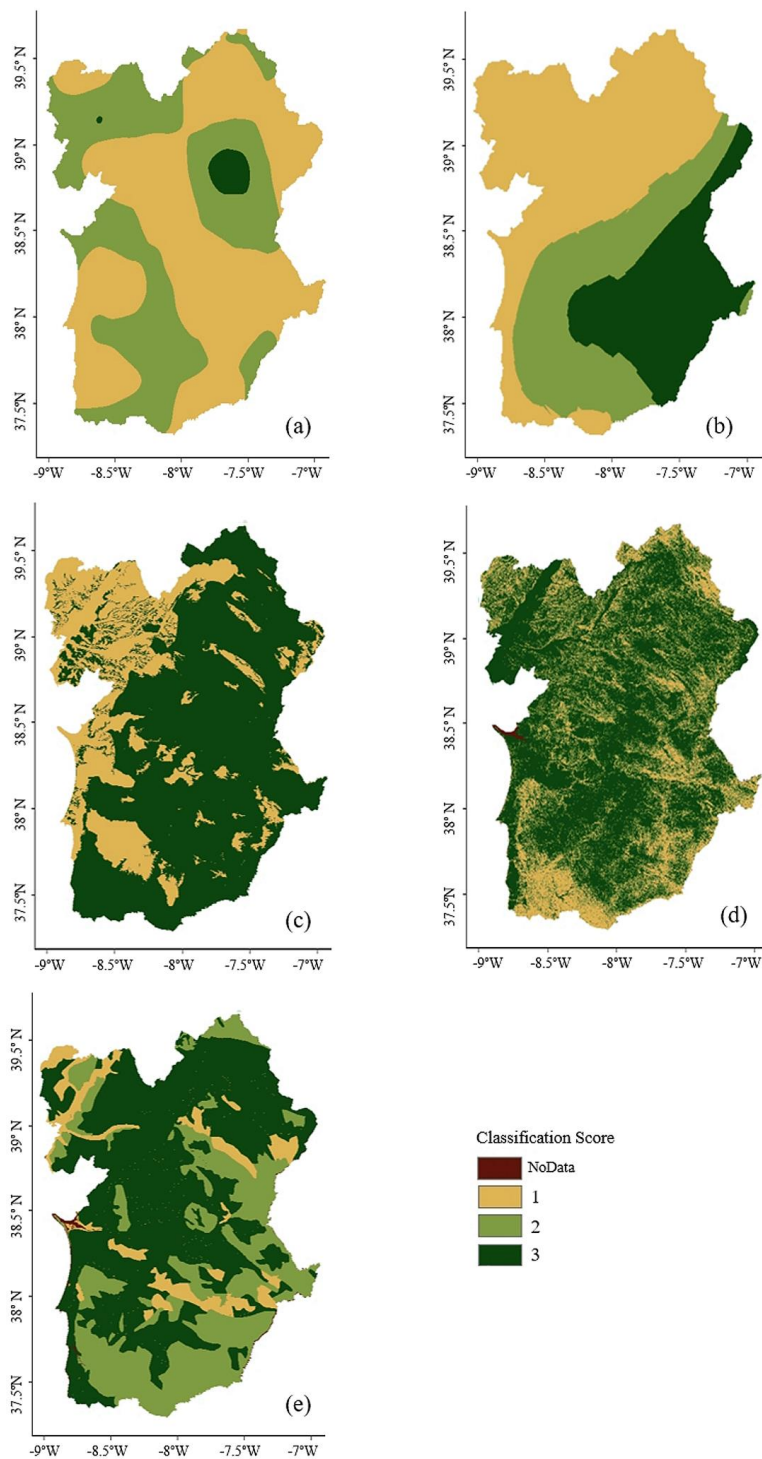
1006 **Figure A2: Correlation plot between predictors used for fitting the simple linear model and the GWR model. AI**
 1007 **is Aridity Index; Depth is Groundwater Depth (Depth) and Ios4 is the Ombrothermic Index of the summer**
 1008 **quarter and the immediately previous month.**

1009

1010



1011 **Appendix B**



1012



1013 **Figure B1 – Predictors maps after classification. (a) – Ombrothermic Index of the summer quarter and the**
1014 **immediately previous month (Ios4); (b) – Aridity Index (AI); (c) – Groundwater Depth (Depth); (d) – Slope;**
1015 **(e) – Soil type.**

1016

1017

1018

1019

1020

1021

1022